HHS Public Access

Author manuscript

ACS Nano. Author manuscript; available in PMC 2020 January 22.

Published in final edited form as:

ACS Nano. 2019 January 22; 13(1): 38–53. doi:10.1021/acsnano.8b06164.

Improved Efficacy and Reduced Toxicity Using a Custom-Designed Irinotecan-Delivering Silicasome for Orthotopic Colon Cancer

Xiangsheng Liu[1,2,⊥], **Jinhong Jiang**[2,⊥], **Ryan Chan**[1], **Ying Ji**[1], **Jianqin Lu**[1,2], **Yu-Pei Liao**[1], **Michael Okene**[1], **Joshua Lin**[1], **Paulina Lin**[1], **Chong Hyun Chang**[2], **Xiang Wang**[2], **Ivanna Tang**[1], **Emily Zheng**[1], **Waveley Qiu**[1], **Zev A. Wainberg**[3], **Andre E. Nel**[1,2,4,*], and **Huan Meng**[1,2,4,*]

[1]Division of Nanomedicine, Department of Medicine, University of California, Los Angeles, California 90095, United States

[2]Center for Environmental Implications of Nanotechnology, California NanoSystems Institute, University of California, Los Angeles, California 90095, United States

[3]Department of Medicine, University of California, Los Angeles, California 90095, United States

[4]California NanoSystems Institute, University of California, Los Angeles, California 90095, United States

Abstract

Irinotecan is a key chemotherapeutic agent for the treatment of colorectal (CRC) and pancreatic (PDAC) cancer. Because of a high incidence of bone marrow and gastrointestinal (GI) toxicity, Onivyde® (a liposome) was introduced to provide encapsulated irinotecan (Ir) delivery in PDAC patients. While there is an ongoing clinical trial (NCT02551991) to investigate the use of Onivyde® as a 1st-line option to replace irinotecan in FOLFIRINOX, the liposomal formulation is currently prescribed as a 2nd-line treatment option (in combination with 5-fluorouracil and leucovorin) for patients with metastatic PDAC who failed gemcitabine therapy. However, the toxicity of Onivyde® remains a concern that needs to be addressed for use in CRC as well. Our goal was to custom design a mesoporous silica nanoparticle (MSNP) carrier for encapsulated irinotecan delivery in a robust CRC model. This was achieved by developing an orthotopic tumor chunk model in immunocompetent mice. With a view to increase the production volume and to expand the disease applications, the carrier design was improved by using an ethanol exchange method for coating of a supported lipid bilayer (LB) that entraps a protonating agent. The encapsulated protonating agent was subsequently used for remote loading of irinotecan. The excellent irinotecan loading capacity and stability of the LB-coated MSNP carrier, also known as a "silicasome", previously showed improved efficacy and reduced toxicity when compared to an in-

*To whom correspondence should be addressed: hmeng@mednet.ucla.edu, anel@mednet.ucla.edu.
⊥X. S. Liu and J. H. Jiang contributed equally to this work.

Competing financial interests: The authors declare the following competing financial interest(s): Andre E. Nel and Huan Meng are co-founders and equity holders in Westwood Bioscience Inc. The remaining authors declare no conflict of interest.

Supporting Information Available: Additional figures, table, and methods as described in the text. This material is available free of charge *via* the Internet at http://pubs.acs.org.

house liposomal carrier in a PDAC model. Intravenous injection of the silicasomes in a well-developed orthotopic colon cancer model in mice demonstrated improved pharmacokinetics and tumor drug content over free drug and Onivyde®. Moreover, improved drug delivery was accompanied by substantially improved efficacy, increased survival and reduced bone marrow and GI toxicity compared to the free drug and Onivyde®. We also confirmed that the custom-designed irinotecan silicasomes outperform Onivyde® in an orthotopic PDAC model. In summary, the Ir-silicasome appears to be promising as a treatment option for CRC in humans based on improved efficacy and the carrier's favorable safety profile.

Graphical Abstract

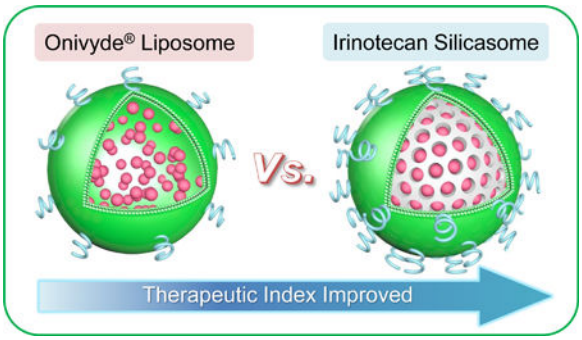

Keywords

irinotecan; silicasome; mesoporous silica nanoparticles; supported lipid bilayer; colorectal cancer; pancreatic cancer; Onivyde®

Irinotecan, a topoisomerase I inhibitor, is frequently used for chemotherapy in gastrointestinal (GI) cancers, including colorectal cancer (CRC) and pancreatic ductal adenocarcinoma (PDAC).[1–6] Most commonly, irinotecan is used in combination with infusion fluorouracil (5-FU) and leucovorin (LV) as a 1st-line treatment option for metastatic CRC.[4,5] It was also suggested that irinotecan can serve as a monotherapy for CRC patients who are unable to tolerate 5-FU.[5,7] In spite of its efficacy, irinotecan use is hindered by high drug toxicity, with especially severe impact on the bone marrow (*e.g.,* neutropenia) and the GI tract (*e.g.,* diarrhea).[8,9] As a result, irinotecan-based chemotherapy is generally conserved for patients with good performance status who tolerate the side effects. This restricts its use in poor performance status patients, who are often in need of cytotoxic therapy.

The high rate of irinotecan toxicity has prompted the development of alternative treatment strategies to reduce the drug's serious side effects. This includes the use of encapsulated drug delivery by various nanocarriers, including liposomes (*e.g.,* FDA approved MM-398 for PDAC and IHL-305 in a phase I clinical trial for advanced solid tumors), polymeric nano-conjugates (*e.g.,* NKTR102 in phase III for metastatic breast cancer) and hyaluronic acid nano-complexes (HyACT™ in phase II for colorectal cancer).[10–18] The liposomal carrier, Onivyde® (also known as MM-398 or PEP02), was approved in 2015 for combination with 5-FU/LV as a 2nd-line therapeutic option for patients with metastatic PDAC who progressed after gemcitabine monotherapy, based on an overall survival

improvement of ~2 months.[19–21] However, this approval was accompanied by a “black box” safety warning from the Food and Drug Administration (FDA), citing the possibility of severe and life-threatening neutropenia (grades 3–4, 27%) and severe diarrhea (grades 3–4, 13%).[21] Although Onivyde® also demonstrated antitumor efficacy and improved safety in a subcutaneous CRC model in nude mice,[10] the advantages of encapsulated drug delivery could not be demonstrated in CRC patients in a phase II clinical trial, and the effort was abandoned.[22] Nonetheless, Onivyde® is currently being tested in variety of solid tumor types, including lung and breast cancer.[23,24]

We have recently demonstrated the utility of a first-generation mesoporous silica nanoparticle (MSNP) drug carrier for irinotecan delivery in an orthotopic PDAC model, with improved efficacy and reduced toxicity compared to an in-house liposome.[14] MSNPs are excellent carriers due to high biocompatibility, large surface area, tunable particle/pore sizes and tunable surface functionalization.[14,25–37] It was also demonstrated that the MSNPs are biodegradable to silicic acid that is eliminated *via* urinary and fecal secretion in mice.[38–40] Since the improved efficacy of our lipid bilayer (LB)-coated MSNP carrier, *a.k.a.* silicasome, has been ascribed to improved drug loading capacity and LB stability over the liposome,[14] we were interested in testing a next- generation silicasome carrier in a murine orthotopic colon cancer model. The design improvement was necessitated by the demand for an increased production volume for clinical translation as well as expanding the use of the carrier for other disease applications. In addition to redesigning the synthesis of the bare MSNPs by a multi-parametric approach, it was also necessary to develop an ethanol exchange method for coating the surface of the MSNPs with a LB, in light of the logistical limitations of using a biofilm for encapsulation. In order to perform the study in a reproducible preclinical CRC model, we also developed a rigorous and reproducible orthotopic tumor chunk model in mice. Our data will show that the improved pharmacokinetics (PK) and tumor irinotecan levels of the silicasome is accompanied by increased efficacy compared to free drug or Onivyde®. We will also show that the silicasome substantially reduces bone marrow and GI toxicity compared to other treatment modalities. We further confirmed that the next generation silicasomes outperforms Onivyde® in an orthotopic PDAC model.

Results

Customized design of the irinotecan silicasome for comparative studies

In order to streamline silicasome production for a comprehensive series of comparative studies in orthotopic animal models other than PDAC, it was necessary to scale up the synthesis of the particles by eliminating the use of a lipid biofilm method to coat the particles.[14,35] Since the surface area of the lipid biofilm is a limiting factor for synthesizing large particle batches (as explained in supplementary data and Figures. S1A-C), it was necessary to substitute this procedure by a custom-designed approach that uses an ethanol exchange procedure as described in Figure 1.[14,35] The ethanol exchange method involved the direct introduction of the bare MSNP, suspended in an aqueous solution, into a concentrated ethanol-dissolved lipid solution, followed by sonication (Figures 1C and S1D-E).[28,41] This approach allowed us to increase the LB coated batch size from a few hundred

milligrams up to ~100 g batch sizes (Figure S1E). Increased batch sizes also demanded optimization of the sol-gel reaction parameters for MSNP synthesis, as described online in Figures S2-4. This involved a multiparameter design process in which the reaction temperature, reaction time, stirring speed and the ratio of silica precursor (tetraethyl orthosilicate, TEOS) *vs.* the organic base (triethanolamine, TEA-ol) and templating agent (cetyltrimethylammonium chloride, CTAC) were varied in a combinatorial fashion. After experimenting with ~70 reaction conditions in an iterative design process, it was possible to accomplish ~100 g batch sizes in ~18 L reaction volume (Figure 1D). The particles were of the desired particle size, pore structure and size, surface area and pore volume as shown in Figures 1D and S5. We demonstrated that extensive washing in ethanol/HCl and pure ethanol can effectively remove the CTAC, which is capable of exerting cytotoxic effects and activation of pro-inflammatory responses (Figures 1D and S6). The absence of cytotoxicity and pro-inflammatory effects of the bare particles were demonstrated *in vitro* in a variety of cell lines, using particle doses up to 1,000 μg/mL (Figures S7 and S8).

To prepare a 20 g batch of silicasomes for the performance of experimentation in this communication, we followed the steps outlined in Figure 1A. Briefly, MSNP (40 mg/mL) was incubated in a solution containing the trapping agent triethylammmonium sucrose octasulfate (TEA_8SOS), and then mixed with 500 mg/mL lipid ethanol solution at the ratio of 1:10 (v/v, ethanol: H_2O). The remaining steps for making the drug-laden particles included the removal of the free TEA_8SOS, remote irinotecan loading, purification and sterilization as described in the methods section (Figure 1A). A schematic depicting the principles for remote drug loading is shown in Figure S9. The final product was referred as the “Ir-silicasome”. Physicochemical characteristics of Ir-silicasome vs Onivyde® are summarized in Figure 1E. This includes the hydrodynamic size measurement by DLS, which demonstrated a hydrodynamic size of ~110 nm and ~130 nm for Ir-silicasome and Onivyde® respectively. The Ir-silicasome sample was also visualized by CryoEM, and compared to the morphology of Onivyde® (Figure 1E). This allowed us to obtain primary particle sizes and standard deviation by viewing at least 100 randomly selected particles in each of the Ir-silicasome and Onivyde® formulations. CryoEM data showed primary sizes of 78.0 ± 6.8 nm for the silicasome and 67.1 ± 19.7 nm for Onivyde®, respectively. CryoEM also revealed that although the silicasome particles were of uniform size (Figure 1E), Onivyde® contained a mixture of large and small liposomal vesicles of uni-or multi-lamellar composition. This is reflected by the coefficient of variation index (CV%) of 29.4% for Onivyde® *vs.* 8.7% for the Ir-silicasome.[42] Other physicochemical characteristics, including loading capacity, hydrodynamic size, zeta potential, endotoxin level and sterility, are shown in Figure 1E.

The cytotoxic potential of the newly synthesized Ir-silicasome was tested by an MTS assay in a variety of cancer cells. This demonstrated that the silicasome could provide increased MC38 and KPC cell killing compared to the liposomal irinotecan carrier (Figure S10). The free drug exhibited the most robust killing effect, a finding that is frequently seen in comparative analyses of free *vs* encapsulated chemotherapy agents *in vitro*.[43,44] One explanation is that the free drug is more rapidly taken up into the cytosol while the encapsulated drug carriers need to be internalized, followed by more gradual drug release to the cytosol and the nucleus.

Establishing a robust orthotopic model for colon cancer

In order to establish a rigorous orthotopic model for colon cancer, the classic approach of injecting MC38 cells into the wall of the cecum in C57BL/6 mice had to be changed since the procedure was only successful in ~40% of mice in our hands due to uncertainty about the exact depth of tumor cell injection into the wall (Figure S11).[45] To improve the tumor engraftment rate, we developed an orthotopic model, in which tumor chunks were fastened to the cecum wall by a stitch.[46] The tumor chunks were obtained from subcutaneous growth of MC38 tumors in C57BL/6 mice (Figure 2A). This approach helped to establish successful orthotopic tumor growth in >95% animals, while also avoiding seepage of bowel content from the cecum to the peritoneum. Hematoxylin and eosin (H&E) staining of a biopsy taken from the primary attachment site demonstrated the presence of orthotopic tumor invasion into the cecal wall (Figure 2B). Using luciferase-expressing MC38 cells (MC38-luc) to non-invasively monitor orthotopic tumor growth by IVIS imaging, it was possible to discern a primary tumor mass within a week (Figure 2C), whereupon exponential growth ultimately leads to metastatic spread and the occurrence of ascites, leading to a moribund state within 4 weeks (Figure 2D).

Pharmacokinetic profile and irinotecan levels in the orthotopic MC38 tumors

The pharmacokinetic (PK) studies were performed in healthy C57BL/6 mice, which received a single intravenous (IV) injection of the silicasome to deliver an irinotecan dose of 40 mg/kg. Onivyde® and the free drug, used at equivalent doses, were used as controls. A dose of 40 mg/kg was chosen based on literature that this is equal to ~2/3 of the free irinotecan maximal tolerated dose (MTD) in mice.[10,14,47] Plasma samples collected at different time points were used to quantify the irinotecan concentration in plasma, using UPLC-MS. The PK data were fitted in a one-compartment model, using PKSolver software.[48] These calculations demonstrated that the circulatory half-life ($t_{1/2}$) of Ir-silicasome was ~9.6 h compared to ~3.3 h for Onivyde® (Figure 3A). Free irinotecan was rapidly cleared from the circulation, with a $t_{1/2}$ of < 30 min. The detailed PK parameters are summarized in Table S1. Please notice that our PK data did not include the measurement of SN-38, which is the active metabolite into which the irinotecan is converted at the tumor site.[9] While published human data for Onivyde® has demonstrated that it was possible to detect an SN-38 concentration that was ~7800-fold less than the measurable blood content of irinotecan (*i.e.,* SN-38 C_{max} of ~ 9.2 ng/mL *vs* 72 μg/mL for irinotecan),[49] it was not possible to detect SN-38 in the limited blood volumes that could be obtained from mice (where the lowest level of detection was ~30 ng/mL).

The drug biodistribution to the MC38 orthotopic tumor site was determined by injecting a dose equivalent of 40 mg/kg irinotecan intravenously, followed by animals sacrifice after 48 and 72 h. Drug delivery by the silicasome resulted in a ~55-fold and ~2.8-fold higher drug content at the tumor site compared to free drug and Onivyde® at 48 hr, respectively (Figure 3B). The comparable increases after 72 h were ~63-fold and ~5.3-fold, respectively (Figure 3B). Utilizing near infrared (NIR) labeled silicasomes,[14,50] we could also follow carrier biodistribution by IVIS fluorescence imaging of explanted tumor tissue and organs (Figure 3C). This demonstrated that the particles showed abundant distribution to the primary tumor site, liver and spleen, with some fluorescence associated with the kidneys. A semi-

quantitative display of NIR image intensity is shown in Figure S12. These results were also confirmed by coupled plasma optical emission spectrometry (ICP-OES) to display Si abundance, demonstrating that ~5% of the injected dose (ID) distributed to the orthotopic tumor site after 48 h (Figure 3D). It was also possible to view the NIR-labeled silicasomes at the tumor site by confocal microscopy (Figure 3E). We found a heterogeneous particle distribution in the tumor microenvironment, with a relatively high particle density in the vicinity of the $CD31^+$ tumor blood vessels (Figure 3E). This is compatible with the previous demonstration of the micro-heterogeneity of MSNP distribution in pancreatic and breast cancer xenograft tumor sites.[51,52]

Prolonged animal survival in the CRC orthotopic tumor model during treatment with the Ir-silicasome

Treatment efficacy and animal survival were determined in the orthotopic tumor model by IV injection of an irinotecan dose equivalent of 40 mg/kg free drug, Ir-silicasomes or Onivyde® every third or fourth day, as shown in Figure 4A (upper panel). Tumor growth (n = 6) was monitored by IVIS imaging up to day 21, where the appearance of peritoneal metastases and ascites interfered in quantifying the bioluminescence intensity (Figure 4A, bottom left).[53] Quantitative display of the imaging data was shown in the bottom right panel in Figure 4A, which demonstrated clear tumor inhibition by the Ir-silicasome. Noteworthy, no significant tumor growth inhibition was seen in mice receiving identical doses and frequency of free drug or Onivyde® administration. Continued daily monitoring of the animals to the point of moribund health status or spontaneous animal death, allowed us to generate comparative survival data.[50,54] Data expression by Kaplan-Meier plots and Log-rank testing (SPSS software)[55,56] demonstrated a statistically significant survival benefit ($p < 0.05$) for the Ir-silicasome as compared to saline, free irinotecan, and Onivyde® (Figure 4B). However, no significant survival benefit was seen for free irinotecan or Onivyde®.

A repeat of the efficacy experiment (n = 3) to harvest tumor tissue 24 h after the 4^{th} IV injection, allowed us to generate quantitative data for tumor weight and histological characteristics (Figure 4C). This demonstrated a significant reduction in tumor weight for the silicasome *vs.* free drug or Onivyde® (Figure 4C). Moreover, we also confirmed using immunohistochemistry (IHC) staining for cleaved caspase-3 (CC-3), differences in the rate of apoptosis amongst the treatment groups (Figure 4D). Thus, while the rate of apoptosis was ~16% for the Ir-silicasome treated group, the values were ~2.5% and ~6.5% for free drug and Onivyde®, respectively.

Major toxicity reduction in the bone marrow and the GI tract, as a result of silicasome use

Irinotecan exerts major systemic toxicological effects (*e.g.,* neutropenia and diarrhea) when used as a free drug monotherapy or in combination with 5-FU (*i.e.,* FOLFIRI regimen) in CRC.[2–4] This constitutes one of the principal reasons for considering encapsulated irinotecan delivery. To study acute bone marrow toxicity, we designed the toxicity study based on a literature-recommended protocol where the mice were sacrificed at 24 h after receiving six daily irinotecan IV injections to allow for the detection of acute myelosuppression and overall change in health status.[57–59] Thus, an independent experiment was performed in C57BL/6 mice receiving an initial plus three follow-up doses of 40 mg/kg

irinotecan IV injections (Figure 5A).[59] The possibility of acute myelosuppression effects was assessed by the collection of whole blood 24 h after the last IV injection, as well as looking at bone marrow cellularity.[59] No effect was seen on animal weight (Fig S13), while assessment of differential WBC counts demonstrated a significant degree of neutropenia in animals treated with free irinotecan or Onivyde® (Figure 5A, left panel). The toxicity was reduced by treating with the Ir-silicasome, which yielded essentially a normal neutrophil count compared to the saline group. Sternums were collected to evaluate bone marrow cellularity by H&E staining (Figure 5B). While both the free drug and Onivyde® exhibited significant myelosuppressive effects as evidenced by estimation of total marrow cellularity or the presence of nucleated hematopoietic cells,[59] no obvious change in cellularity was observed in Ir-silicasome treated animals (Figure 5B). The visual appearance was confirmed by computer software that semi-quantitatively scored the total marrow cellularity and hematopoietic nuclei in the histology images (Figure 5A).[60] Thus, while the total and hematopoietic cellularity were reduced by ~26% and ~44% in the Onivyde® treated group, the corresponding values were ~0% and ~3% in the Ir-silicasome treated group.

In addition to the bone marrow assessment, sections of the small bowel were used to evaluate the presence of apoptotic cells in the intestinal crypts, using IHC to detect cleaved caspase-3 (Figure 5C).[61] This demonstrated a significant reduction in the number of $CC\text{-}3^{+}$ cells in animals treated with the silicasome carrier compared to the free drug and Onivyde® (Figure 5 D). Curiously, we did not observe significant liver toxicity by any of the treatment modules in C57BL/6 mice, which differs from the higher rates of toxicity seen in a previous study in B6129SF1/J mice (Figure S14).[14,62,63] All considered, the aforementioned data demonstrate that the custom-designed Ir-silicasome carrier provides favorable toxicity reduction compared to free irinotecan and Onivyde®.

Confirmation of the efficacy of the next-generation Ir-silicasome in a PDAC model

The first silicasome generation provided an effective anti-tumor effect free irinotecan in an orthotopic animal model. In order to see how the efficacy of the newly synthesized silicasome compare to Onivyde®, we made use of the $Kras^{LSL\text{-}G12D/+}$/$Trp53^{LSL\text{-}R172H/+}$/Pdx-1-Cre (KPC) derived PDAC model,[14] which is explained in Figure S15. Assessment of tumor drug content demonstrated that the Ir-silicasome could provide a ~5.3-fold and ~48-fold increase in the PDAC drug content compared to Onivyde® and free drug, after 48 h, respectively (Figure 6A). The differences were even more significant after 72 h, amounting to ~8.7-fold and ~79-fold increases, respectively (Figure 6A). Therapeutic efficacy was assessed at either a fixed time point (Figure 6B) or when the tumor-bearing mice approached moribund status (Figure 6C). The IVIS imaging data and CC-3 IHC results showed that the Ir-silicasome significantly reduced primary tumor growth and suppression of metastases (Figures 6B and S16). While free irinotecan led to inefficient tumor inhibition on primary tumor growth and metastasis, Onivyde® had a modest impact on both parameters. Clearly, the Ir-silicasome had the most robust effect on apoptosis at the PDAC site compared to other treatments (Figure 6B and S17). The use of Kaplan-Meier analysis in a survival experiment also demonstrated a significantly increased lifespan ($p = 0.047$) through the use of the Ir-silicasome compared to Onivyde® (Figure 6C, left panel). This effect is also reflected by the comparative IVIS imaging data shown in Figure 6C (right panel) and quantification of

bioluminescence intensity in the operator-defined region of interest at the tumor sites (Figure S18).

Discussion

In this communication, we demonstrated that the use of a custom-designed irinotecan-delivering silicasome can improve drug delivery in an orthotopic colon cancer model, leading to an improved treatment outcome and significant toxicity reduction compared to the free drug and Onivyde®. Our data demonstrate that the improved PK of the silicasome was accompanied by at least an order of magnitude increase in the drug concentration at the tumor site compared to free irinotecan. The improved drug biodistribution was accompanied by dramatic tumor shrinkage and increased tumor cell death. Moreover, the silicasome also outperformed the Onivyde® liposome with respect to PK properties, tumor drug levels, and efficacy, particularly at later time points. Additionally, there were also clear differences between the nanocarriers in terms of adverse outcomes in the bone marrow and GI tract. We also demonstrated that the increased efficacy of the silicasome in the colon model could be reproduced in PDAC, similar to the previous comparative study with a first generation silicasome *vs.* an in-house liposome.[14] Based on these observations, we propose that the Ir-silicasome could also be considered as a treatment option for colon cancer, where the reduction of irinotecan toxicity, coupled with improved efficacy, could advance the Ir-silicasome to be more frequently considered as a treatment consideration for encapsulated drug delivery.

Although liposomal irinotecan has been approved as a 2nd-line treatment option for PDAC, a Phase II clinical trial using Onivyde® for CRC treatment yielded disappointing results, leading to temporary abandonment of the therapeutic effort for this cancer indication.[22] However, it should be possible to revisit the option of irinotecan monotherapy for CRC with the development of our newly designed Ir-silicasome carrier. We should also consider the use of the Ir-silicasome as a substitute for free irinotecan in GI cancer treatment combinations such as FOLFIRINOX (5-FU, folinic acid, irinotecan, oxaliplatin), FOLFIRI (5-FU, folinic acid, irinotecan), XELIRI (irinotecan, capecitabine), FOLFIRI plus the vascular endothelial growth factor (VEGF) antibody, bevacizumab, or the epidermal growth factor (EGFR) antibody, cetuximab.[4,5,64,65] This being stated, it is important to consider that each of these treatment options involve consideration of specific variables that may be introduced by individual treatments, *e.g.,* normalization of blood vessels by VGEF blockage, which could impact permeability and egress to the tumor site.[66] This could have a bearing on the efficacy of various carrier characteristics such as size and the ability of the particle to change its shape during egress through the blood vessel wall.[66–68] Recently, a modified FOLFIRINOX (mFOLFIRINOX) regimen, which adjusts the 5-FU and irinotecan dosing schedule, has attracted attention due to a significant disease-free survival improvement compared to gemcitabine (21.6 *vs.* 12.8 months) in non-metastatic PDAC.[69] It is possible that the silicasome can further improve these therapeutic combinations, in addition to the major effect on the irinotecan toxicity reduction.

In this study, a key discovery is the increased potency of the Ir-silicasome compared to Onivyde® in two orthotopic tumor models. An obvious advantage is the improved PK and

tumor drug content of the silicasome over the liposome. This improved performance is derived from the structural composition and design features of the silicasome compared to the liposome. First, the support provided by the mesoporous silica core allows improved stability of the LB compared to that of the liposome.[14,27–29,70] This stability improvement is reflected by prolonged circulatory half-life. Second, the porous structure of the coated MSNP provide a large surface area for drug packaging against the side walls of the pores as result of electrostatic and *van der Waals* interactions.[26,31,32] Thus, the large internal surface area of the MSNPs (~800 m^2/g) allows more drug encapsulation than for a liposome of equal size. This feature also accounts for the slower drug release rate from the Ir-slicasome compared to Onivyde® under abiotic testing conditions (Figure S19). A third major differential feature from a formulation perspective, is the increased PEG2000 density of the Ir-silicasome (3 mol%) *vs.* Onivyde® (0.3 mol%). In a simulation study, it was demonstrated that the PEG2000 chain assumed a hemispherical ("mushroom") conformation on the lipid bilayer at low density (*e.g.,* <1.6 mol%).[71] However, at higher PEG grafting density, the PEG2000 molecules exhibit an extended "brush" conformation, which is associated with reduced plasma protein binding to the nanoparticle surface under experimental and simulation conditions.[71–74] Based on the quantitative assessment of the Flory radius or grafting point distance for PEG in the literature,[71] we propose that the PK data could reasonably be interpreted to imply that the 3 mol% PEG density in silicasome assumes a brush-like confirmation that reduces mononuclear phagocyte system (MPS) uptake, leading to a prolonged circulatory $t_{1/2}$.[73,75–79] In contrast, the simulation studies for PEG2000 would suggest that the lesser 0.3 mol% PEG density of the liposome assumes a "mushroom" shape, which is associated with faster clearance from the blood.[71] Collectively, the combination of improved stability, large internal surface area and increased PEGylation density of the silicasome likely contributes to the improved PK and tumor drug content during treatment with this carrier.

Finally, a major benefit of using the silicasome *vs.* the liposome for irinotecan delivery in PDAC and colon cancer is toxicity reduction in the bone marrow and the gastrointestinal tract, as demonstrated in our study. This is in agreement with a previous PDAC study (performed before the commercial availability of Onivyde®) in which we demonstrated that the silicasome could outperform an in-house liposome due to reduced irinotecan leakage and a slower rate of drug release.[14] One possible explanation is the decreased rate of premature drug release from the silicasome due to increased lipid bilayer stability. Another explanation for the differential toxicity could be the differences in the level of PEGylation of the carriers, which could allow increased opsonization of the lesser PEGylated liposomal membrane to lead to increased phago-endocytosis by the reticuloendothelial cells in the myeloid bone marrow.[80] From this perspective, it has been demonstrated in imaging studies that 60 nm PEG-coated nanoparticles are capable of being phago-endocytosed by bone marrow reticuloendothelial cells and released across the capillary wall into the myeloid bone marrow interstitium.[80–82] It is possible that the carrier size and the deformability of the carrier could possibly play a role in favoring liposome over silicasome uptake in the bone marrow, leading to increased toxicity.

Conclusions

In summary, we demonstrated the establishment of a next generation silicasome proved to be more efficacious with reduced toxicity during Irinotecan delivery to orthotopic CRC and PDAC models. Since Onivyde® resulted in a disappointing outcome in a phase II clinical study in CRC, the availability of an alternative carrier, which can be produced in large quantities, could allow the pursuit of human clinical studies with the silicasome in patients with CRC, in addition to the potential treatment benefit in PDAC. Moreover, the silicasome nanocarrier can also be used to deliver other chemotherapeutic agents, such as weak basic drugs that can be remotely loaded into the carrier, including the ability to co-encapsulate synergistic drug combinations.

Methods

Materials

Tetraethylorthosicate (TEOS), triethanolamine (TEA-ol), (3-aminopropyl)triethoxysilane (APTES), cetyltrimethylammonium chloride solution (CTAC, 25 wt% in water) and Dowex 50WX8 resin were purchased from Sigma-Aldrich, USA. Sucrose octasulfate (SOS) sodium salt was purchased from Toronto Research Chemicals, Inc, Canada. Triethylamine (TEA) was purchased from Acros, USA. Sepharose CL-4B was purchased from GE Healthcare, USA. Irinotecan hydrochloride trihydrate was purchased from LC Laboratories, USA. Onivyde® (Ipsen Biopharmaceuticals, Inc., 4.3 mg/mL irinotecan free base, 10 mL/vial) was purchased through the UCLA health pharmacy. 1,2-Distearoyl-sn-glycero-3-phosphocholine (DSPC), 1,2-distearoyl-sn-glycero-3-phosphoethanol amine-N-[methoxy(polyethylene glycol)-2000] (ammonium salt) (DSPE-PEG_{2000}), and cholesterol (Chol) were purchased from Avanti Polar Lipids, USA. Penicillin, streptomycin, Dulbecco's modified Eagle medium (DMEM) and Roswell Park Memorial Institute (RPMI) 1640 medium were purchased from Invitrogen. Fetal bovine serum (FBS) was purchased from Gemini Bio Products. Rabbit mAb antibody (catlog. #9664), which detects activated (cleaved) caspase-3, was purchased from Cell Signaling. Anti-CD31 antibody (catalog# 553708) was purchased from BD Pharmingen™, USA. Alexa Fluor® 488 conjugated goat anti-rabbit IgG (H+L) secondary antibody (catalog# A11008), and DyLight 680 NHS ester were purchased from Thermo Fisher Scientific Inc, USA. Matrigel™ Matrix Basement Membrane was purchased from BD Bioscience.

Synthesis, purification, and characterization of Ir-silicasomes

Synthesis of bare MSNPs: 17.1 L pure water was added to a 20 L beaker. 0.9 L CTAC solution (25 wt.% in H_2O) was gently added while stirring at 185 rpm, using an overhead stirrer shaft. The solution was heated to 85 °C while stirring and then 72 g triethanolamine in 300 mL H_2O was added when the solution reached a temperature of 85 °C. After stirring the solution for another 30 min at 85°C, 600 mL TEOS at 85 °C was gently added, followed by stirring at the same temperature for another ~4 hr. This yielded a milky particle suspension, which was allowed to cool down naturally to room temperature. Six L of ethanol was added to the suspension to precipitate the silica particles, followed by centrifugation at 10,000 rpm for 10 mins. To remove the CTAC, the particles pellets were resuspended in acidic ethanol

(HCl/ethanol, 4:100 v/v) by sonication through repeated centrifugation (10,000 rpm x 60 mins) and resuspension, which was repeated 5 times. This was followed by washing in pure ethanol 3 times. The primary size and morphology of the particles were characterized using TEM (JEOL 1200-EX). The presence of residual CTAC in the MSNP was tested by FTIR and high-performance liquid chromatography (HPLC, Infinity 1260, Agilent), using an Acclaim Surfactant Plus column. A charged aerosol detector was used for CTAC quantification. Surface area, pore volume, and pore size of the purified MSNP were tested by (Brunauer-Emmett-Teller) BET measurement, as described before.[50]

Lipid coating using an ethanol exchange method: Briefly, a mixture of lipids (16 g DSPC, 5.4 g, cholesterol (Chol) and 2.8 g DSPE-PEG_{2000}, yielding a DSPC/Chol/DSPE-PEG_{2000} molar ratio of 3:2:0.15) was dissolved in 50 mL pure ethanol at ~65°C. 500 mL of a preheated (~65°C) solution, containing a 40 mg/mL MSNP suspension into which 80 mM TEA_8SOS trapping agent was soaked, was poured into the lipid solution while stirring at ~1,000 rpm. The TEA_8SOS trapping agent was made based on our established protocol.[14] The mixture was treated by probe sonication (power = 200 W) using a 15s/5s on/off cycle for 2 hr. In between, the sample was stirred at ~500 rpm, followed by centrifugation at 4,000 rpm for 5 min to remove any aggregates.

Removal of free TEA_8SOS and remote loading of the irinotecan into the silicasomes: Unentrapped free TEA_8SOS was removed by size exclusion chromatography over a Sepharose CL-4B column, using a HEPES-buffered dextrose solution (5 mM HEPES, 5% dextrose, pH 6.5) for elution. 10 g irinotecan was dissolved in 1 L HEPES buffered dextrose (5 mM HEPES, 5% dextrose, pH = 6.5) and mixed with the TEA_8SOS-loaded silicasome suspension. The mixture was incubated at ~65 °C for 30 min, before quenching the sample in ice water for ~30 min. The drug loaded silicasome were washed 3 times using a HEPES-buffered NaCl solution (4.05 mg/mL HEPES, 8.42 mg/mL NaCl, pH 7.2). The supernatant was collected and filtered with a 0.45 μm syringe filter, followed by a 0.2 μm filter for sterilization.

Characterization of the Ir-silicasomes

The irinotecan concentration was determined by either UV spectroscopy (360 nm) or HPLC. The free base form of the drug was prepared at 4.3 mg/mL. MSNP mass and lipid mass in the final product were determined by TGA and HPLC, respectively. Particle hydrodynamic size and zeta potential were measured by a ZETAPALS instrument (Brookhaven Instruments Corporation). The DLS size measurement was performed by diluting the MSNP to ~100 μg/mL in DI water. The zeta potential was assessed by diluting the particles in 10 mM NaCl solution, at a concentration of 100 μg/mL. The final product was visualized by cryoEM (TF20 FEI Tecnai-G2 in CNSI) to confirm the uniformity and integrity of the coated lipid bilayer. Endotoxin levels were tested using a chromogenic LAL assay (QCL-1000 300 Test Kit, Lonza). Sterilization of the final product was confirmed by performing tests for microbial contamination (HPC Count sampler, Millipore Corp., MHPC10025) or the presence of yeasts and molds (Yeast and mold sampler, Millipore Corp., MY0010025).

Cell culture

The dimethylhydrazine-induced murine MC38 colon adenocarcinoma cell line,[83] which is syngeneic for a C57BL/6 background, was kindly provided by Dr. Siwen Hu-Lieskovan at UCLA. The KPC murine pancreatic adenocarcinoma cell line was derived from a spontaneous tumor originating in a transgenic $Kras^{LSL\text{-}G12D/+}$; $Trp53^{LSL\text{-}R172H/+}$; Pdx-1-Cre mouse (B6/129 background).[14] To allow bioluminescence tumor imaging, both cells were permanently transfected with a luciferase-based lentiviral vector in the UCLA vector core facility, followed by a limiting dilution cloning.[14,35] Detailed cell culture conditions, cytotoxicity, testing and screening for IL-1β release are described in Supplementary Materials.

Development of an orthotopic MC38 tumor chunk transplantation model

Female C57BL/6 mice were purchased from Charles River Laboratories and maintained under pathogen-free conditions. All animal experiments were performed according to protocols approved by the UCLA Animal Research Committee. In order to prepare a tumor that can be sliced into tumor chunks, MC38-luc cells were subcutaneously injected (~2×10^6 cells suspended in 100 μL of DMEM/Matrigel, 1:1 v/v) in the flank of C57BL/6 mice (6~8 weeks). The mice were euthanized when the tumor size reached ~1 cm^3. The tumor was removed under sterile conditions and cut into ~1.5 mm × ~3 mm tumor chunks.[46] The orthotopic placement of the tumor chunks involved a short surgical procedure in anesthetized (isoflurane, ketamine and xylazine) C57BL/6 mice (10~12 weeks). We also administered the 1^{st} dose of pain medication (carprofen 5 mg/kg, subcutaneous) pre-operatively. The surgical area (abdomen) was shaved with a #40 blade and sterilized with betadine and 70% ethanol. The animals were placed on a heat pad and sterilely draped with gauze to expose the surgical site. A 2–3 cm abdominal incision was made to expose the cecum, which was exteriorized and isolated from the rest of the abdominal content by packed gauze. Warm saline was used to keep the cecum moist. A figure of 8 stitch was placed superficially in the cecum wall, using size 6–0 absorbable sutures (PDS II, Ethicon). The tumor piece was tied onto the wall, which was lightly abraded with tweezers to facilitate tissue level contact with the tumor chunk. After attaching the tumor chunk, the cecum was returned to the abdominal cavity. The inner (fascial) layer was closed with size 6–0 absorbable sutures (PDS II, Ethicon) and the exterior skin was closed with size 5–0 sized non-absorbable sutures (PROLENE, Ethicon). The mice were kept on the warming pads until full recovery from anesthesia, and then transferred to clean cages. The efficacy study was performed in the tumor-bearing mice approximately one week after implantation, at which point the tumors had grown to ~0.5 cm. For the biodistribution experiments, the tumor-bearing mice were used ~2 weeks after tumor implantation, at which point the tumors had grown to a size of ~1.0 cm. The orthotopic implantation of KPC cells in the pancreas of B6/129 mice have been previously described[14,50] and is briefly summarized in the Supplementary Materials.

Assessment of irinotecan pharmacokinetics (PK), using the silicasome

The PK study was performed on 10~12 week old healthy female C57BL/6 mice. The animals received IV injections of free irinotecan, Onivyde® or Ir-silicasome at an irinotecan

dose of 40 mg/kg, followed by collection of blood samples at 5 min, 3, 6, 24, and 48 hrs. After separation of the plasma fraction, the drug was extracted in an acidic methanol solution (0.1 mol/L phosphoric acid/methanol, 1:4 v/v).[14] The irinotecan concentration was measured by UPLC-MS (Waters LCT Premier ESI), using gradient elution of acetonitrile in water at a flow rate of 1.00 mL/min.[84] The PK data were analyzed by PKSolver software, using a one-compartment model.[48]

Tumor drug content and intratumoral biodistribution

Drug content was determined in the tumor tissue obtained from both the MC38 and KPC orthotopic models. Tumor bearing mice received IV injections of free irinotecan, Onivyde® or Ir-silicasome at dose of 40 mg/kg irinotecan. Animals were sacrificed after 48 and 72 hr for collection of tumor tissue, estimation of tumor weight, and homogenization in acidic methanol to measure the drug concentration by UPLC-MS.[14,84] To track the silicasome biodistribution by IVIS imaging, silicasomes were labeled with NIR dye by modifying the MSNP with APTES to react with NHS-DyLight 680 NHS ester,[14,50] following which tumor-bearing mice were IV injected with 100 mg/kg MSNP. Animals were sacrificed after 48 hr to collect tumor tissue and major organs for performance of *ex vivo* IVIS imaging and assessment of Si content by ICP-OES. Tumor slices were also cryo-embedded in OCT reagent to prepare tumor sections for confocal microscopy (SP8-SMD, Leica). The tumor blood vessels were stained with a primary anti-CD31 antibody (1:500), followed by an Alexa Fluor® 488-conjugated secondary antibody (1:500). DAPI was used to localize the cellular nuclei.

Assessment of treatment efficacy in the orthotopic tumor models

Seven days after MC38 tumor chunk implantation, the tumor-bearing mice were randomly assigned into 4 groups (n = 6) (Figure 4A-B). Animals in each group received IV injections of free irinotecan, Onivyde®, or Ir-silicasome at an irinotecan dose equivalent of 40 mg/kg, twice per week for a total of 4 to 6 administrations (depending on animal survival). Saline was used as a negative control. To assess survival rate, animals were monitored daily up to the point of spontaneous death or approaching moribund status.[50,54] Live bioluminescence imaging was used to monitor the orthotopic tumor burden twice per week, as previously described.[14] We also performed an efficacy study in the orthotopic MC38 model to obtain tumor tissue for weighing and histological analysis (Figure 4C-D). This study was conducted using a total of four injections as described above, followed by sacrifice on day 18 (24 hr after the 4th IV injection). The orthotopic tumors were harvested and weighed, then fixed in 10% formalin for H&E or assessment of cleaved caspase 3 (CC-3) expression by IHC staining in the UCLA Translational Pathology Core Laboratory. (TPCL). The images were assessed by using Aperio ImageScope software (Leica). The efficacy study in PDAC orthotopic model was provided online.

Safety assessment of encapsulated *versus* free irinotecan delivery

To compare the toxicity of different irinotecan formulations, a toxicity study was performed in healthy female C57BL/6 mice using a published protocol.[59] Animals received daily IV injections of different irinotecan formulations at a drug dose of 40 mg/kg. A total of four administrations were performed.[59] The mice were sacrificed 24 hr after the final injection.

Blood was drawn to perform complete blood count and sternums and other organs collected for histological analysis and IHC. IHC staining to assess CC-3 expression in the small intestine was performed as described above. H&E staining to assess bone marrow and hematopoietic cellularity in the sternum was analyzed by Aperio ImageScope software.[60]

Statistical analysis

Comparative analysis of differences between groups was performed using the 2-tailed Student's *t*-test (Excel software, Microsoft) for two-group comparison. A One-way ANOVA followed by a Tukey's test (Origin software, OriginLab) was performed for multiple group comparisons. Data were expressed as mean ± SD or SEM, as stated in the figure legends. The survival analysis was performed by Log Rank testing (Mantel-Cox) using SPSS 20.0 software. The software instructions for the Log Rank testing indicate that multiple comparisons analysis is possible, including pairwise comparisons for three or more groups. A statistically significant difference was considered at $p < 0.05$.

Supplementary Material

Refer to Web version on PubMed Central for supplementary material.

Acknowledgements

This study was supported by the U.S. Public Health Service Grant, 1U01CA198846. We thank Drs. Siwen Hu-Lieskovan and Antoni Ribas at UCLA for providing the MC38 cell line. We acknowledge use of the IVIS imaging facilities in the Preclinical Imaging Technology Center, the Translational Pathology Core Laboratory (TPCL) for histology H&E and IHC staining, the Electron Imaging Center for Nanomachines (EICN) for CryoEM, the Molecular Instrumentation Center for UPLC-MS, and the CNSI Advanced Light Microscopy/Spectroscopy (ALMS) Shared Facility for confocal fluorescent microscopy at UCLA.

References

(1). Bleiberg H CPT-11 in Gastrointestinal Cancer. Eur. J. Cancer 1999, 35, 371–379. [PubMed: 10448285]

(2). Cunningham D; Pyrhönen S; James RD; Punt CJ; Hickish TF; Heikkila R; Johannesen TB; Starkhammar H; Topham CA; Awad L; Jacques C; Herait P Randomised Trial of Irinotecan plus Supportive Care versus Supportive Care Alone after Fluorouracil Failure for Patients with Metastatic Colorectal Cancer. The Lancet 1998, 352, 1413–1418.

(3). Rougier P; Van Cutsem E; Bajetta E; Niederle N; Possinger K; Labianca R; Navarro M; Morant R; Bleiberg H; Wils J; Awad L; Herait P; Jacques C Randomised Trial of Irinotecan versus Fluorouracil by Continuous Infusion after Fluorouracil Failure in Patients with Metastatic Colorectal Cancer. The Lancet 1998, 352, 1407–1412.

(4). Saltz LB; Cox JV; Blanke C; Rosen LS; Fehrenbacher L; Moore MJ; Maroun JA; Ackland SP; Locker PK; Pirotta N; Elfring GL; Miller LL; Irinotecan plus Fluorouracil and Leucovorin for Metastatic Colorectal Cancer. N. Engl. J. Med. 2000, 343, 905–914. [PubMed: 11006366]

(5). Fuchs C; Mitchell EP; Hoff PM Irinotecan in the Treatment of Colorectal Cancer. Cancer Treat. Rev 2006, 32, 491–503. [PubMed: 16959432]

(6). Conroy T; Desseigne F; Ychou M; Bouché O; Guimbaud R; Bécouarn Y; Adenis A; Raoul J-L; Gourgou-Bourgade S; de la Fouchardière C; Bennouna J; Bachet J-B; Khemissa-Akouz F; Péré-Vergé D; Delbaldo C; Assenat E; Chauffert B; Michel P; Montoto-Grillot C; Ducreux M FOLFIRINOX versus Gemcitabine for Metastatic Pancreatic Cancer. N. Engl. J. Med 2011, 364, 1817–1825. [PubMed: 21561347]

(7). Ychou M; Raoul JL; Desseigne F; Borel C; Caroli-Bosc FX; Jacob JH; Seitz JF; Kramar A; Hua A; Lefebvre P; Couteau C; Merrouche Y High-Dose, Single-Agent Irinotecan as First-Line

Therapy in the Treatment of Metastatic Colorectal Cancer. Cancer Chemother. Pharmacol 2002, 50, 383–391. [PubMed: 12439596]

(8). Hecht JR Gastrointestinal Toxicity of Irinotecan. Oncology 1998, 12, 72–78. [PubMed: 9726096]

(9). Mathijssen RH; van Alphen RJ; Verweij J; Loos WJ; Nooter K; Stoter G; Sparreboom A Clinical Pharmacokinetics and Metabolism of Irinotecan (CPT-11). Clin. Cancer Res 2001, 7, 2182–2194. [PubMed: 11489791]

(10). Drummond DC; Noble CO; Guo Z; Hong K; Park JW; Kirpotin DB Development of a Highly Active Nanoliposomal Irinotecan Using a Novel Intraliposomal Stabilization Strategy. Cancer Res 2006, 66, 3271–3277. [PubMed: 16540680]

(11). Khalid A; Persano S; Shen H; Zhao Y; Blanco E; Ferrari M; Wolfram J Strategies for Improving Drug Delivery: Nanocarriers and Microenvironmental Priming. Expert Opin. Drug Deliv 2017, 14, 865–877. [PubMed: 27690153]

(12). Li F; Zhao X; Wang H; Zhao R; Ji T; Ren H; Anderson GJ; Nie G; Hao J Multiple Layer-by-Layer Lipid-Polymer Hybrid Nanoparticles for Improved FOLFIRINOX Chemotherapy in Pancreatic Tumor Models. Adv. Funct. Mater 2015, 25, 788–798.

(13). Li J; Liu F; Gupta S; Li C Interventional Nanotheranostics of Pancreatic Ductal Adenocarcinoma. Theranostics 2016, 6, 1393–1402. [PubMed: 27375787]

(14). Liu X; Situ A; Kang Y; Villabroza KR; Liao Y; Chang CH; Donahue T; Nel AE; Meng H Irinotecan Delivery by Lipid-Coated Mesoporous Silica Nanoparticles Shows Improved Efficacy and Safety over Liposomes for Pancreatic Cancer. ACS Nano 2016, 10, 2702–2715. [PubMed: 26835979]

(15). Luo D; Carter KA; Lovell JF Nanomedical Engineering: Shaping Future Nanomedicines: Nanomedical Engineering. Wiley Interdiscip. Rev. Nanomed. Nanobiotechnol 2015, 7, 169–188. [PubMed: 25377691]

(16). Pelaz B; Alexiou C; Alvarez-Puebla RA; Alves F; Andrews AM; Ashraf S; Balogh LP; Ballerini L; Bestetti A; Brendel C; Bosi S; Carril M; Chan WCW; Chen C; Chen X; Chen X; Cheng Z, Cui D, Du J, Dullin C; et al. Diverse Applications of Nanomedicine. ACS Nano 2017, 11, 2313–2381. [PubMed: 28290206]

(17). Wang AZ; Langer R; Farokhzad OC Nanoparticle Delivery of Cancer Drugs. Annu. Rev. Med 2012, 63, 185–198. [PubMed: 21888516]

(18). Han H; Valdepérez D; Jin Q; Yang B; Li Z; Wu Y; Pelaz B; Parak WJ; Ji J Dual Enzymatic Reaction-Assisted Gemcitabine Delivery Systems for Programmed Pancreatic Cancer Therapy. ACS Nano 2017, 11, 1281–1291. [PubMed: 28071891]

(19). Chiang N-J; Chang J-Y; Shan Y-S; Chen L-T Development of Nanoliposomal Irinotecan (Nal-IRI, MM-398, PEP02) in the Management of Metastatic Pancreatic Cancer. Expert Opin. Pharmacother 2016, 17, 1413–1420. [PubMed: 27140876]

(20). Passero FC; Grapsa D; Syrigos KN; Saif MW The Safety and Efficacy of Onivyde (Irinotecan Liposome Injection) for the Treatment of Metastatic Pancreatic Cancer Following Gemcitabine-Based Therapy. Expert Rev. Anticancer Ther 2016, 16, 697–703. [PubMed: 27219482]

(21). Wang-Gillam A; Li C-P; Bodoky G; Dean A; Shan Y-S; Jameson G; Macarulla T; Lee K-H; Cunningham D; Blanc JF; Hubner RA; Chiu C-F; Schwartsmann G; Siveke JT; Braiteh F; Moyo V; Belanger B; Dhindsa N; Bayever E; Von Hoff DD; et al. Nanoliposomal Irinotecan with Fluorouracil and Folinic Acid in Metastatic Pancreatic Cancer after Previous Gemcitabine-Based Therapy (NAPOLI-1): A Global, Randomised, Open-Label, Phase 3 Trial. The Lancet 2016, 387, 545–557.

(22). Chibaudel B; Maindrault-Gœbel F; Bachet J-B; Louvet C; Khalil A; Dupuis O; Hammel P; Garcia M-L; Bennamoun M; Brusquant D; Tournigand C; André T; Arbaud C; Larsen AK; Wang Y-W; Yeh CG; Bonnetain F; de Gramont A PEPCOL: A GERCOR Randomized Phase II Study of Nanoliposomal Irinotecan PEP02 (MM-398) or Irinotecan with Leucovorin/5-Fluorouracil as Second-Line Therapy in Metastatic Colorectal Cancer. Cancer Med 2016, 5, 676–683. [PubMed: 26806397]

(23). Zhang H Onivyde for the Therapy of Multiple Solid Tumors. Onco Targets Ther 2016, 20, 3001–3007.

(24). Wu D; Si M; Xue H-Y; Wong HL Nanomedicine Applications in the Treatment of Breast Cancer: Current State of the Art. Int. J. Nanomedicine 2017, 12, 5879–5892. [PubMed: 28860754]

(25). Trewyn BG; Slowing II; Giri S; Chen H-T; Lin VS-Y Synthesis and Functionalization of a Mesoporous Silica Nanoparticle Based on the Sol–Gel Process and Applications in Controlled Release. Acc. Chem. Res 2007, 40, 846–853. [PubMed: 17645305]

(26). Slowing I; Viveroescoto J; Wu C; Lin V Mesoporous Silica Nanoparticles as Controlled Release Drug Delivery and Gene Transfection Carriers. Adv. Drug Deliv. Rev 2008, 60, 1278–1288. [PubMed: 18514969]

(27). Liu J; Stace-Naughton A; Jiang X; Brinker CJ Porous Nanoparticle Supported Lipid Bilayers (Protocells) as Delivery Vehicles. J. Am. Chem. Soc 2009, 131, 1354–1355. [PubMed: 19173660]

(28). Cauda V; Engelke H; Sauer A; Arcizet D; Rädler J; Bein T Colchicine-Loaded Lipid Bilayer-Coated 50 nm Mesoporous Nanoparticles Efficiently Induce Microtubule Depolymerization upon Cell Uptake. Nano Lett 2010, 10, 2484–2492. [PubMed: 20515041]

(29). Ashley CE; Carnes EC; Phillips GK; Padilla D; Durfee PN; Brown PA; Hanna TN; Liu J; Phillips B; Carter MB; Carroll NJ; Jiang X; Dunphy DR; Willman CL; Petsev DN; Evans DG; Parikh AN; Chackerian B; Wharton W; Peabody DS; et al. The Targeted Delivery of Multicomponent Cargos to Cancer Cells by Nanoporous Particle-Supported Lipid Bilayers. Nat. Mater 2011, 10, 389–397. [PubMed: 21499315]

(30). He Q; Gao Y; Zhang L; Zhang Z; Gao F; Ji X; Li Y; Shi J A pH-Responsive Mesoporous Silica Nanoparticles-Based Multi-Drug Delivery System for Overcoming Multi-Drug Resistance. Biomaterials 2011, 32, 7711–7720. [PubMed: 21816467]

(31). He Q; Shi J Mesoporous Silica Nanoparticle Based Nano Drug Delivery Systems: Synthesis, Controlled Drug Release and Delivery, Pharmacokinetics and Biocompatibility. J. Mater. Chem 2011, 21, 5845.

(32). Tang F; Li L; Chen D Mesoporous Silica Nanoparticles: Synthesis, Biocompatibility and Drug Delivery. Adv. Mater 2012, 24, 1504–1534. [PubMed: 22378538]

(33). Argyo C; Weiss V; Bräuchle C; Bein T Multifunctional Mesoporous Silica Nanoparticles as a Universal Platform for Drug Delivery. Chem. Mater 2014, 26, 435–451.

(34). Zhang Q; Wang X; Li P-Z; Nguyen KT; Wang X-J; Luo Z; Zhang H; Tan NS; Zhao Y Biocompatible, Uniform, and Redispersible Mesoporous Silica Nanoparticles for Cancer-Targeted Drug Delivery In Vivo. Adv. Funct. Mater 2014, 24, 2450–2461.

(35). Meng H; Wang M; Liu H; Liu X; Situ A; Wu B; Ji Z; Chang CH; Nel AE Use of a Lipid-Coated Mesoporous Silica Nanoparticle Platform for Synergistic Gemcitabine and Paclitaxel Delivery to Human Pancreatic Cancer in Mice. ACS Nano 2015, 9, 3540–3557. [PubMed: 25776964]

(36). Alvarez-Berríos MP; Sosa-Cintron N; Rodriguez-Lugo M; Juneja R; Vivero-Escoto JL Hybrid Nanomaterials Based on Iron Oxide Nanoparticles and Mesoporous Silica Nanoparticles: Overcoming Challenges in Current Cancer Treatments. J. Chem 2016, 2016, 1–15.

(37). Singh RK; Patel KD; Leong KW; Kim H-W Progress in Nanotheranostics Based on Mesoporous Silica Nanomaterial Platforms. ACS Appl. Mater. Interfaces 2017, 9, 10309–10337. [PubMed: 28274115]

(38). Lu J; Liong M; Li Z; Zink JI; Tamanoi F Biocompatibility, Biodistribution, and Drug-Delivery Efficiency of Mesoporous Silica Nanoparticles for Cancer Therapy in Animals. Small 2010, 6, 1794–1805. [PubMed: 20623530]

(39). Huang X; Li L; Liu T; Hao N; Liu H; Chen D; Tang F The Shape Effect of Mesoporous Silica Nanoparticles on Biodistribution, Clearance, and Biocompatibility *in Vivo*. ACS Nano 2011, 5, 5390–5399. [PubMed: 21634407]

(40). Liu T; Li L; Teng X; Huang X; Liu H; Chen D; Ren J; He J; Tang F Single and Repeated Dose Toxicity of Mesoporous Hollow Silica Nanoparticles in Intravenously Exposed Mice. Biomaterials 2011, 32, 1657–1668. [PubMed: 21093905]

(41). Hohner AO; David MPC; Rädler JO Controlled Solvent-Exchange Deposition of Phospholipid Membranes onto Solid Surfaces. Biointerphases 2010, 5, 1–8. [PubMed: 20408729]

(42). Rice SB; Chan C; Brown SC; Eschbach P; Han L; Ensor DS; Stefaniak AB; Bonevich J; Vladár AE; Walker ARH; Zheng J; Starnes C; Stromberg A; Ye J; Grulke EA Particle Size Distributions

by Transmission Electron Microscopy: An Interlaboratory Comparison Case Study. Metrologia 2013, 50, 663–678. [PubMed: 26361398]

(43). Eliaz RE; Szoka FC Liposome-Encapsulated Doxorubicin Targeted to CD44: A Strategy to Kill CD44-Overexpressing Tumor Cells. Cancer Res. 2001, 61, 2592–2601. [PubMed: 11289136]

(44). Alyane M; Barratt G; Lahouel M Remote Loading of Doxorubicin into Liposomes by Transmembrane pH Gradient to Reduce Toxicity toward H9c2 Cells. Saudi Pharm. J 2016, 24, 165–175. [PubMed: 27013909]

(45). McIntyre RE; Buczacki SJA; Arends MJ; Adams DJ Mouse Models of Colorectal Cancer as Preclinical Models. BioEssays 2015, 37, 909–920. [PubMed: 26115037]

(46). Tseng W; Leong X; Engleman E Orthotopic Mouse Model of Colorectal Cancer. J. Vis. Exp 2007, 10, 484.

(47). Messerer CL Liposomal Irinotecan: Formulation Development and Therapeutic Assessment in Murine Xenograft Models of Colorectal Cancer. Clin. Cancer Res 2004, 10, 6638–6649. [PubMed: 15475454]

(48). Zhang Y; Huo M; Zhou J; Xie S PKSolver: An Add-in Program for Pharmacokinetic and Pharmacodynamic Data Analysis in Microsoft Excel. Comput. Methods Programs Biomed 2010, 99, 306–314. [PubMed: 20176408]

(49). Chen L; Chang T; Cheng A; Yang C; Shiah H; Chang J; Yeh G Phase I Study of Liposome Encapsulated Irinotecan (PEP02) in Advanced Solid Tumor Patients. J. Clin. Oncol 2008, 26, 2565–2565.

(50). Liu X; Lin P; Perrett I; Lin J; Liao Y-P; Chang CH; Jiang J; Wu N; Donahue T; Wainberg Z; Nel AE; Meng H Tumor-Penetrating Peptide Enhances Transcytosis of Silicasome-Based Chemotherapy for Pancreatic Cancer. J. Clin. Invest 2017, 127, 2007–2018. [PubMed: 28414297]

(51). Meng H; Mai WX; Zhang H; Xue M; Xia T; Lin S; Wang X; Zhao Y; Ji Z; Zink JI; Nel AE Codelivery of an Optimal Drug/siRNA Combination Using Mesoporous Silica Nanoparticles To Overcome Drug Resistance in Breast Cancer *in Vitro* and *in Vivo*. ACS Nano 2013, 7, 994–1005. [PubMed: 23289892]

(52). Meng H; Zhao Y; Dong J; Xue M; Lin Y-S; Ji Z; Mai WX; Zhang H; Chang CH; Brinker CJ; Zink JI; Nel AE Two-Wave Nanotherapy To Target the Stroma and Optimize Gemcitabine Delivery To a Human Pancreatic Cancer Model in Mice. ACS Nano 2013, 7, 10048–10065. [PubMed: 24143858]

(53). Terracina KP; Aoyagi T; Huang W-C; Nagahashi M; Yamada A; Aoki K; Takabe K Development of a Metastatic Murine Colon Cancer Model. J. Surg. Res 2015, 199, 106–114. [PubMed: 26009494]

(54). Olive KP; Jacobetz MA; Davidson CJ; Gopinathan A; McIntyre D; Honess D; Madhu B; Goldgraben MA; Caldwell ME; Allard D; Frese KK; Denicola G; Feig C; Combs C; Winter SP; Ireland-Zecchini H; Reichelt S; Howat WJ; Chang A; Dhara M; et al. Inhibition of Hedgehog Signaling Enhances Delivery of Chemotherapy in a Mouse Model of Pancreatic Cancer. Science 2009, 324, 1457–1461. [PubMed: 19460966]

(55). Kuriyama S; Kikukawa M; Mitoro A; Tsujinoue H; Nakatani T; Yamazaki M; Yoshiji H; Toyokawa Y; Yoshikawa M; Fukui H Antitumor Effect of Electrochemotherapy on Colorectal Carcinoma in an Orthotopic Mouse Model. Int. J. Oncol 1999, 14, 321–6. [PubMed: 9917509]

(56). Kleinbaum DG; Klein M Kaplan-Meier Survival Curves and the Log-Rank Test. In Survival Analysis; Springer New York: New York, NY, 2012; pp 55–96.

(57). Wang Y; Probin V; Zhou D Cancer Therapy-Induced Residual Bone Marrow Injury-Mechanisms of Induction and Implication for Therapy. Curr. Cancer Ther. Rev 2006, 2, 271–279. [PubMed: 19936034]

(58). Feng L; Huang Q; Huang Z; Li H; Qi X; Wang Y; Liu Z; Liu X; Lu L Optimized Animal Model of Cyclophosphamide-Induced Bone Marrow Suppression. Basic Clin. Pharmacol. Toxicol 2016, 119, 428–435. [PubMed: 27061017]

(59). Iusuf D; Ludwig M; Elbatsh A; van Esch A; van de Steeg E; Wagenaar E; van der Valk M; Lin F; van Tellingen O; Schinkel AH OATP1A/1B Transporters Affect Irinotecan and SN-38 Pharmacokinetics and Carboxylesterase Expression in Knockout and Humanized Transgenic Mice. Mol. Cancer Ther 2014, 13, 492–503. [PubMed: 24194565]

(60). Travlos GS Normal Structure, Function, and Histology of the Bone Marrow. Toxicol. Pathol 2006, 34, 548–565. [PubMed: 17067943]

(61). Tian X; Nguyen M; Foote HP; Caster JM; Roche KC; Peters CG; Wu P; Jayaraman L; Garmey EG; Tepper JE; Eliasof S; Wang AZ CRLX101, a Nanoparticle–Drug Conjugate Containing Camptothecin, Improves Rectal Cancer Chemoradiotherapy by Inhibiting DNA Repair and HIF1α. Cancer Res 2017, 77, 112–122. [PubMed: 27784746]

(62). Ahowesso C; Piccolo E; Li XM; Dulong S; Hossard V; La Sorda R; Filipski E; Tinari N; Delaunay F; Iacobelli S; Lévi F Relations between Strain and Gender Dependencies of Irinotecan Toxicity and UGT1A1, CES2 and TOP1 Expressions in Mice. Toxicol. Lett 2010, 192, 395–401. [PubMed: 19931604]

(63). Okyar A; Piccolo E; Ahowesso C; Filipski E; Hossard V; Guettier C; La Sorda R; Tinari N; Iacobelli S; Lévi F Strain- and Sex-Dependent Circadian Changes in Abcc2 Transporter Expression: Implications for Irinotecan Chronotolerance in Mouse Ileum. PLoS ONE 2011, 6, e20393. [PubMed: 21674030]

(64). Hurwitz H; Fehrenbacher L; Novotny W; Cartwright T; Hainsworth J; Heim W; Berlin J; Baron A; Griffing S; Holmgren E; Ferrara N; Fyfe G; Rogers B; Ross R; Kabbinavar F Bevacizumab plus Irinotecan, Fluorouracil, and Leucovorin for Metastatic Colorectal Cancer. N. Engl. J. Med 2004, 350, 2335–2342. [PubMed: 15175435]

(65). Cunningham D; Humblet Y; Siena S; Khayat D; Bleiberg H; Santoro A; Bets D; Mueser M; Harstrick A; Verslype C; Chau I; Van Cutsem E; Cetuximab Monotherapy and Cetuximab plus Irinotecan in Irinotecan-Refractory Metastatic Colorectal Cancer. N. Engl. J. Med 2004, 351, 337–345. [PubMed: 15269313]

(66). Chauhan VP; Stylianopoulos T; Martin JD; Popović Z; Chen O; Kamoun WS; Bawendi MG; Fukumura D; Jain RK Normalization of Tumour Blood Vessels Improves the Delivery of Nanomedicines in a Size-Dependent Manner. Nat. Nanotechnol 2012, 7, 383–388. [PubMed: 22484912]

(67). Jain RK; Martin JD; Stylianopoulos T The Role of Mechanical Forces in Tumor Growth and Therapy. Annu. Rev. Biomed. Eng 2014, 16, 321–346. [PubMed: 25014786]

(68). Shi J; Kantoff PW; Wooster R; Farokhzad OC Cancer Nanomedicine: Progress, Challenges and Opportunities. Nat. Rev. Cancer 2017, 17, 20–37. [PubMed: 27834398]

(69). Conroy T; Hammel P; Hebbar M; Ben Abdelghani M; Wei AC; Raoul J-L; Chone L; Francois E; Artru P; Biagi JJ; Lecomte T; Assenat E; Faroux R; Ychou M; Volet J; Sauvanet A; Jouffroy-Zeller C; Rat P; Castan F; Bachet J-B Unicancer GI PRODIGE 24/CCTG PA.6 Trial: A Multicenter International Randomized Phase III Trial of Adjuvant mFOLFIRINOX versus Gemcitabine (Gem) in Patients with Resected Pancreatic Ductal Adenocarcinomas. J. Clin. Oncol 2018, 36, LBA4001.

(70). Wang F; Liu J Liposome Supported Metal Oxide Nanoparticles: Interaction Mechanism, Light Controlled Content Release, and Intracellular Delivery. Small 2014, 10, 3927–3931. [PubMed: 24861966]

(71). Lee H; Larson RG Adsorption of Plasma Proteins onto PEGylated Lipid Bilayers: The Effect of PEG Size and Grafting Density. Biomacromolecules 2016, 17, 1757–1765. [PubMed: 27046506]

(72). Perry JL; Reuter KG; Kai MP; Herlihy KP; Jones SW; Luft JC; Napier M; Bear JE; DeSimone JM PEGylated PRINT Nanoparticles: The Impact of PEG Density on Protein Binding, Macrophage Association, Biodistribution, and Pharmacokinetics. Nano Lett 2012, 12, 5304–5310. [PubMed: 22920324]

(73). Hak S; Helgesen E; Hektoen HH; Huuse EM; Jarzyna PA; Mulder WJM; Haraldseth O; Davies C. de L. The Effect of Nanoparticle Polyethylene Glycol Surface Density on Ligand-Directed Tumor Targeting Studied in Vivo by Dual Modality Imaging. ACS Nano 2012, 6, 5648–5658. [PubMed: 22671719]

(74). Kumagai M; Sarma TK; Cabral H; Kaida S; Sekino M; Herlambang N; Osada K; Kano MR; Nishiyama N; Kataoka K Enhanced in Vivo Magnetic Resonance Imaging of Tumors by PEGylated Iron-Oxide-Gold Core-Shell Nanoparticles with Prolonged Blood Circulation Properties. Macromol. Rapid Commun 2010, 31, 1521–1528. [PubMed: 21567561]

(75). Li S-D; Huang L Stealth Nanoparticles: High Density but Sheddable PEG Is a Key for Tumor Targeting. J. Controlled Release 2010, 145, 178–181.

(76). Otsuka H; Nagasaki Y; Kataoka K PEGylated Nanoparticles for Biological and Pharmaceutical Applications. Adv. Drug Deliv. Rev 2012, 64, 246–255.

(77). Liu X; Huang N; Wang H; Li H; Jin Q; Ji J The Effect of Ligand Composition on the in Vivo Fate of Multidentate Poly(Ethylene Glycol) Modified Gold Nanoparticles. Biomaterials 2013, 34, 8370–8381. [PubMed: 23932246]

(78). Suk JS; Xu Q; Kim N; Hanes J; Ensign LM PEGylation as a Strategy for Improving Nanoparticle-Based Drug and Gene Delivery. Adv. Drug Deliv. Rev 2016, 99, 28–51. [PubMed: 26456916]

(79). Lucas AT; Herity LB; Kornblum ZA; Madden AJ; Gabizon A; Kabanov AV; Ajamie RT; Bender DM; Kulanthaivel P; Sanchez-Felix MV; Havel HA; Zamboni WC Pharmacokinetic and Screening Studies of the Interaction between Mononuclear Phagocyte System and Nanoparticle Formulations and Colloid Forming Drugs. Int. J. Pharm 2017, 526, 443–454. [PubMed: 28473237]

(80). Sarin H Physiologic Upper Limits of Pore Size of Different Blood Capillary Types and Another Perspective on the Dual Pore Theory of Microvascular Permeability. J. Angiogenesis Res 2010, 2, 14.

(81). Illum L; Davis SS Targeting of Colloidal Particles to the Bone Marrow. Life Sci 1987, 40, 1553–1560. [PubMed: 3561165]

(82). Porter CJH; Moghimi SM; Davies MC; Davis SS; Illum L Differences in the Molecular Weight Profile of Poloxamer 407 Affect Its Ability to Redirect Intravenously Administered Colloids to the Bone Marrow. Int. J. Pharm 1992, 83, 273–276.

(83). Corbett TH; Griswold DP; Roberts BJ; Peckham JC; Schabel FM Tumor Induction Relationships in Development of Transplantable Cancers of the Colon in Mice for Chemotherapy Assays, with a Note on Carcinogen Structure. Cancer Res 1975, 35, 2434–2439. [PubMed: 1149045]

(84). Lu J; Liu X; Liao Y-P; Salazar F; Sun B; Jiang W; Chang CH; Jiang J; Wang X; Wu AM; Meng H; Nel AE Nano-Enabled Pancreas Cancer Immunotherapy Using Immunogenic Cell Death and Reversing Immunosuppression. Nat. Commun 2017, 8, 1811. [PubMed: 29180759]

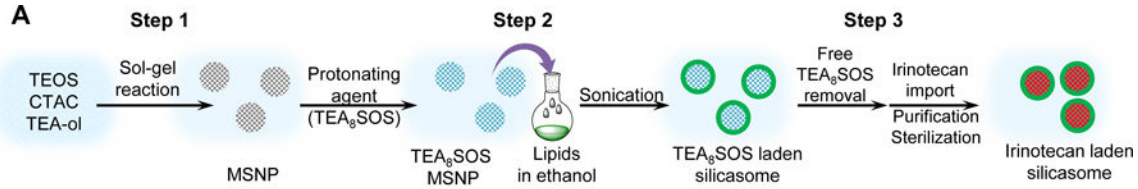

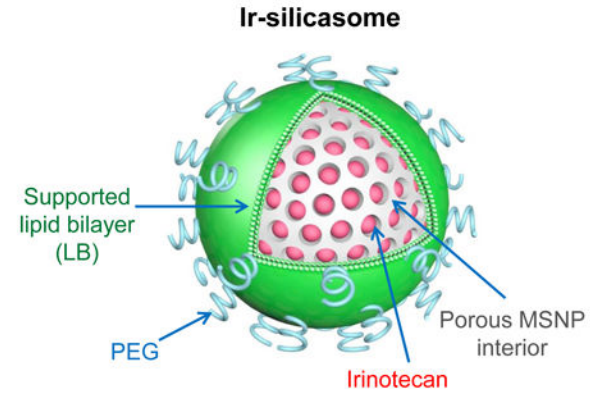

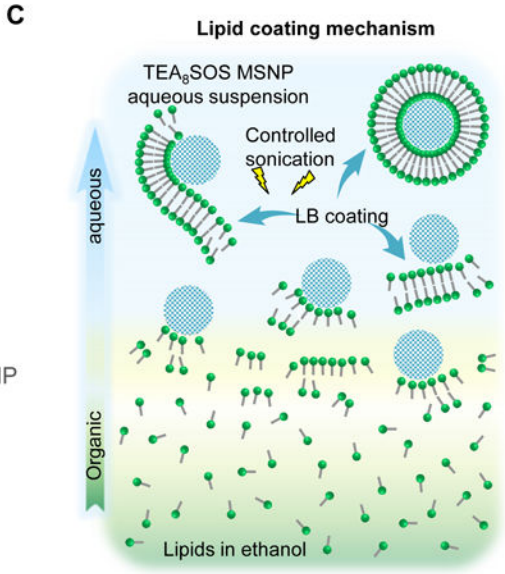

D

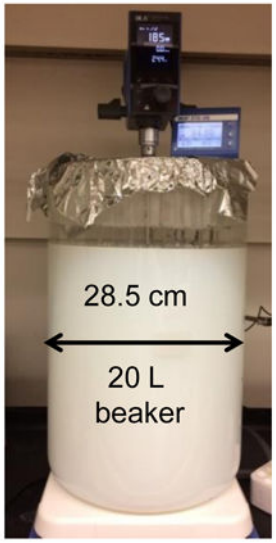

Bare MSNP physicochemical properties	
Primary size	~ 61.9 ± 6.4 nm
Hydrodynamic size (polydispersity index, PDI)	~80 nm (PDI ~ 0.01)
MSNP surface area	~837 m^2/g
MSNP pore volume	~0.977 cm^3/g
MSNP pore size	~3.1 nm
CTAC residue	<0.2% w/w (CTAC/MSNP)
Endotoxin level (at 10 mg/mL)	< 1 EU/ml

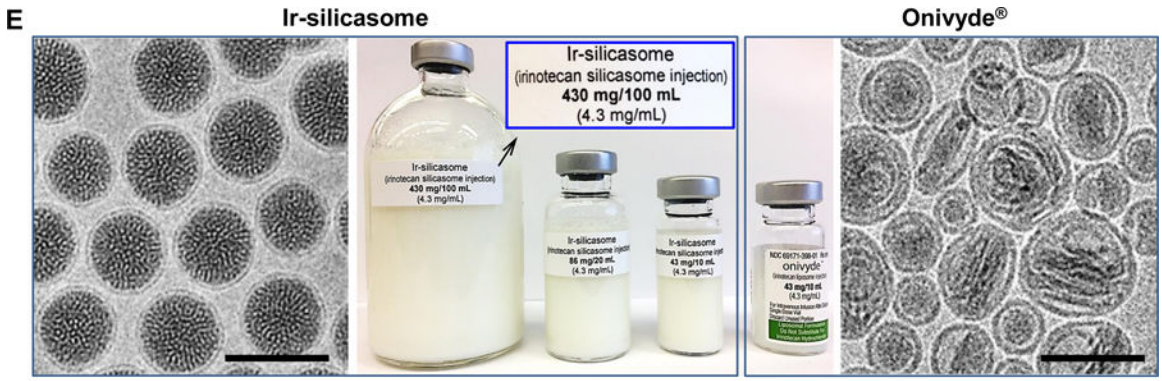

Physicochemical characterization of the final product

	Ir-silicasome	Onivyde®
Primary size (cryo-EM)	78.0±6.8 nm	67.1±19.7 nm
(coefficient of variation, CV%)	(8.7%)	(29.4%)
Hydrodynamic size (polydispersity index)	~130 nm (PDI<0.1)	~110 nm (PDI<0.1)
Zeta potential	~ -11 mV	~ -16 mV
API loading capacity	~40 % (w/w, drug/MSNP)	~55 % (w/w, drug/lipids)
pH	~7.2	~7.2
API concentration	5 mg/mL	5 mg/mL
Unencapsulated drug	< 5%	< 5%
Endotoxin level	< 1 EU/ml	< 1 EU/ml
Sterility testing	Sterile	Sterile

Figure 1. Development of a custom-designed irinotecan silicasome nanocarrier.

(A) Schematic to show the different steps for developing the irinotecan nanocarrier, namely: (1) bare mesoporous silica nanoparticle (MSNP) synthesis and purification (see detailed description of the high-volume process online and Figures S2-8), (2) lipid coating of the particles containing the soaked-in trapping agent, triethylammmonium sucrose octasulfate (TEA_8SOS); and (3) remote loading of irinotecan by a proton gradient (generated by the trapping agent), followed by purification and sterilization. (**B**) The final product, the Ir-silicasome, is comprised of a MSNP core that contains a large packaging space for irinotecan, which is stably entrapped by a lipid bilayer (LB). The LB contains a PEG attachment to improve colloidal stability and circulatory half-life. **(C)** Schematic to show the custom-designed procedure for surface coating by an alcohol-exchange method. Lipids are dissolved in ethanol as described in the online data section Figure S1. This ethanol suspension is rapidly mixed with TEA_8SOS laden particles and sonicated, which leads to the lipids assembling on the particle surface, and rapid sealing of the pores. **(D)** The integrated synthesis process, with precise control of temperature, stirring speed, and addition of the precursor materials at optimal ratios, is capable of producing 18 L batches that contain ~100 g of particles, as described online. The table shows the physicochemical properties of the purified bare MSNPs. **(E)** CryoEM visualization of the Ir-silicasome and Onivyde®. The final Ir-silicasome product contains an irinotecan (free base) concentration of 4.3 mg/mL, which was dispensed in smaller volumes in glass containers. The table summarizes the comparative physicochemical properties.

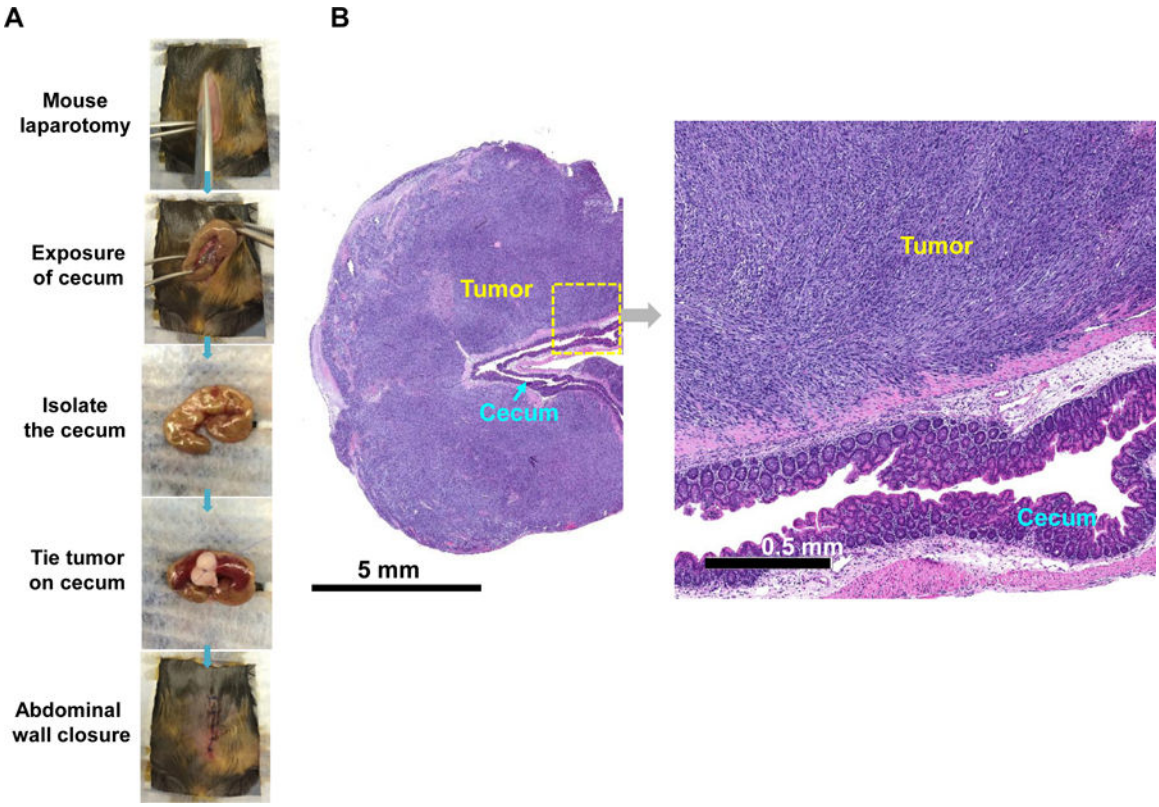

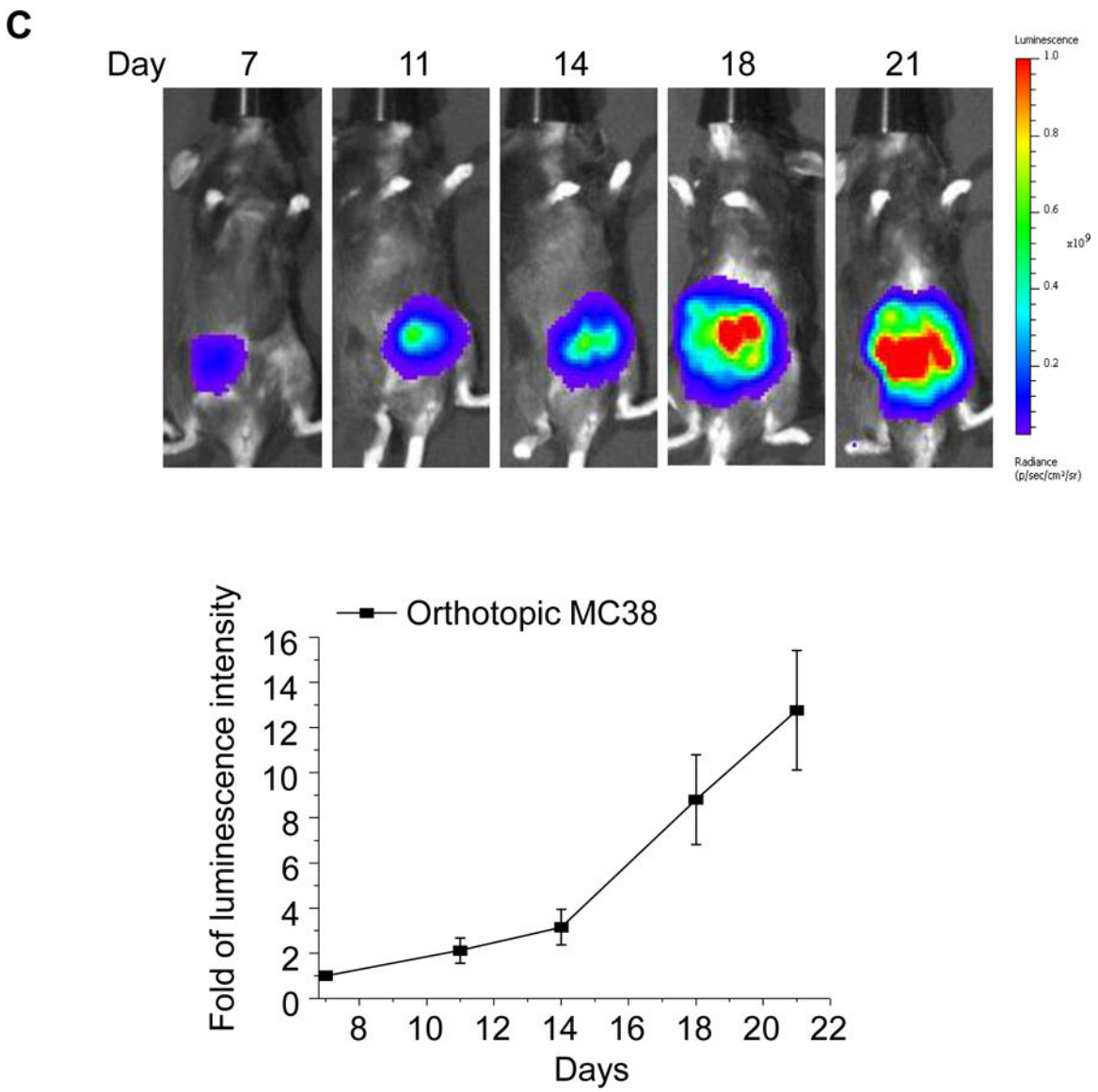

D

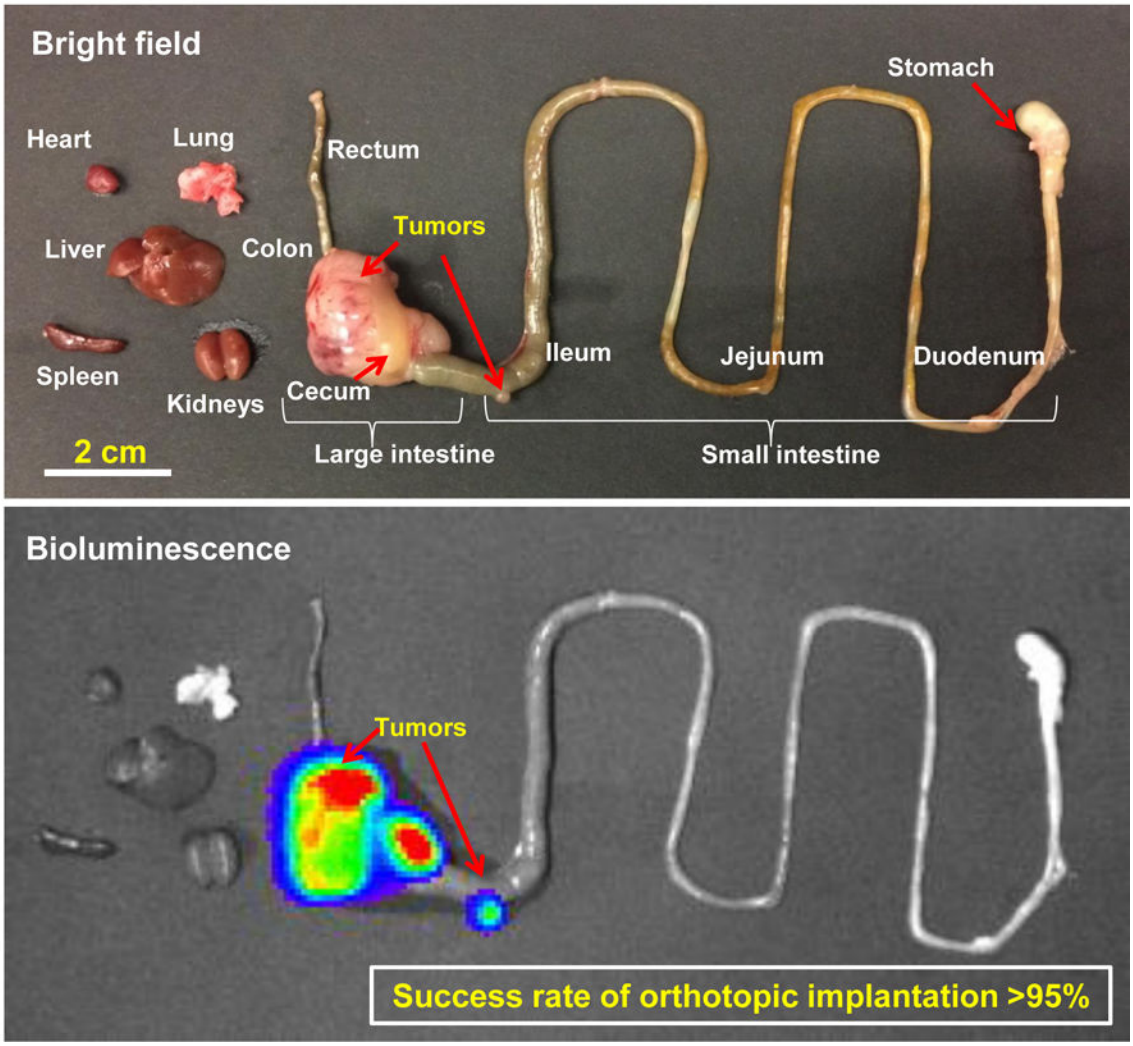

Figure 2. Establishment of an orthotopic MC38-luc tumor chuck model in C57BL/6 mice.

(A) The orthotopic implantation involves minor surgery to place the MC38 tumor chunks on the cecum wall of C57BL/6 mice. Briefly, the tumor chunks were obtained from subcutaneous growing tumors established in C57BL/6 mice. Once the tumor reached ~1 cm in size, the tumor mass was aseptically harvested and cut up into 2~4 mm^3 chunks. These tumor chunks were tied onto the cecum wall by absorbable surgical sutures. **(B)** H&E staining to show the growth of the orthotopic tumor in relation to the adjacent normal tissue. **(C)** Live-animal IVIS imaging to monitor the orthotopic tumor growth. The bioluminescence intensity was quantified at the region of interest (ROI) by IVIS Living Image software. **(D)** Example *ex vivo* IVIS image of the complete gastrointestinal tract of an animal, sacrificed ~3 weeks post tumor chunk implantation. More than 95% of operated mice developed primary tumors, which metastasized to adjacent intestinal tissues and the peritoneum.

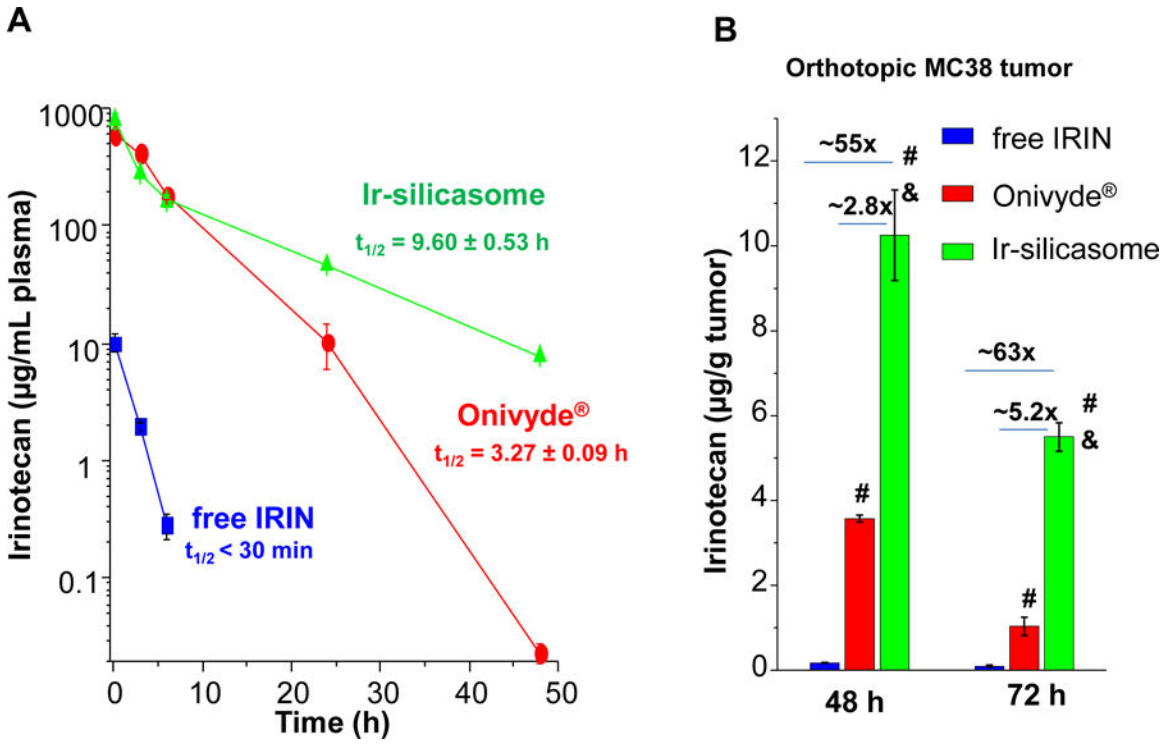

C

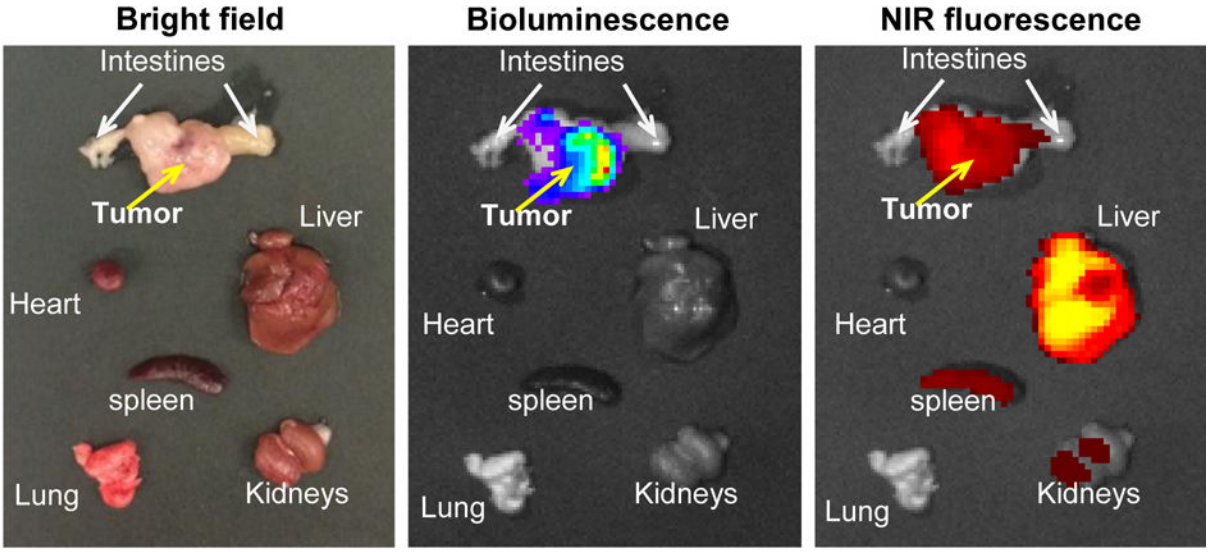

D

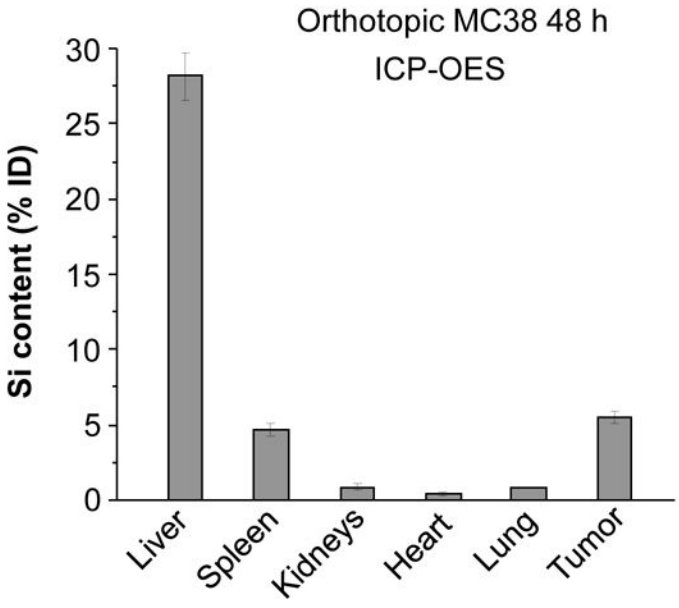

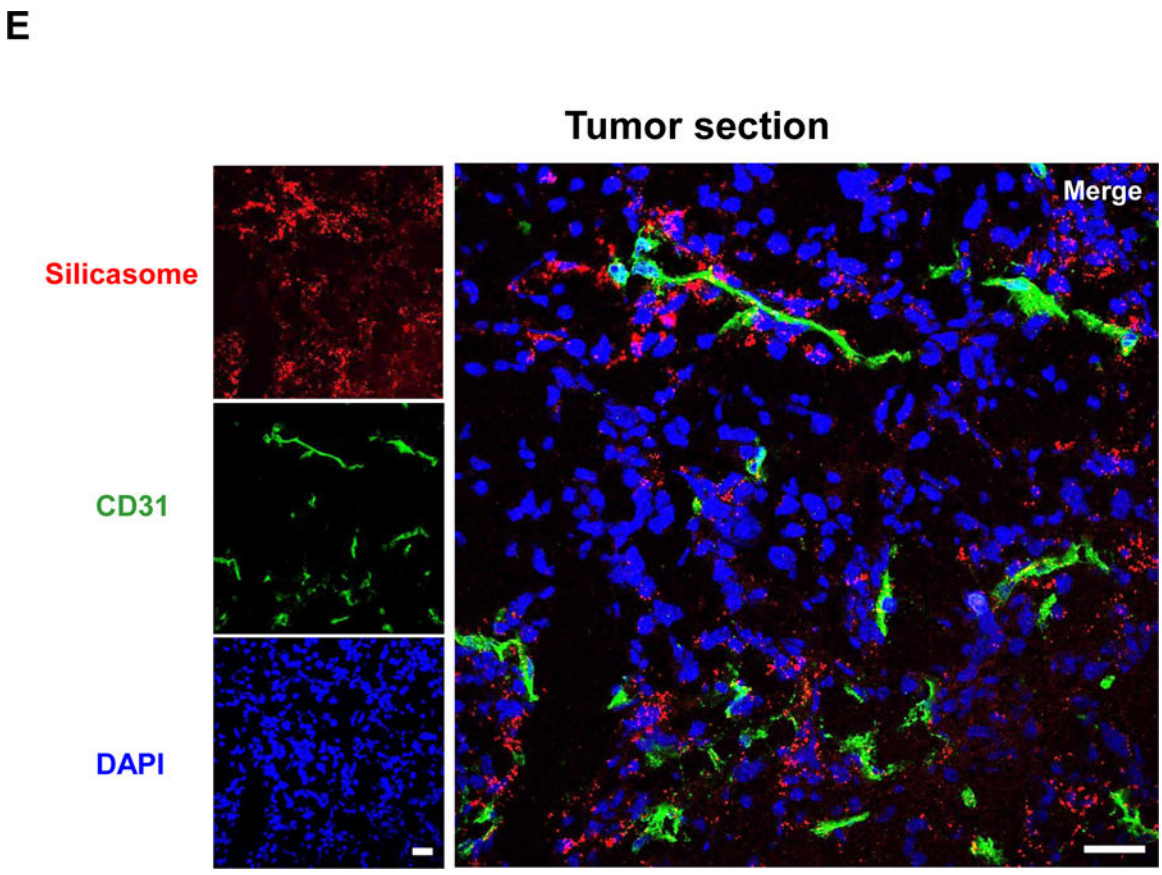

Figure 3. Improved PK and tumor irinotecan concentrations using the silicasome carrier for treating orthotopic tumor-bearing mice.

(A) PK profile after a single IV injection of free drug or the nanocarriers at an irinotecan (IRIN) dose equivalent of 40 mg/kg (n = 3). Circulatory $t_{1/2}$ values were calculated using PKSolver software. **(B)** Drug content at the tumor site after 48 hr and 72 hr in animals receiving an IV injection of 40 mg/kg irinotecan by the different carriers. (**C**) *Ex vivo* IVIS imaging of tumor-bearing mice receiving IV injection of DyLight680-labeled silicasomes at the identical dose in (A). Tumor tissue and major organs were harvested at 48 hr. (**D**) ICP-OES was used to quantify the percent injected Si dose (%ID) at the different sites after 48 hr. (**E**) Confocal microscopy to show the intratumoral distribution of the NIR silicasome particles used in the same experiment as in (C). Color code: Red, NIR silicasome particles; green, blood vessel staining with anti-CD31 antibody; blue, nuclear stained with DAPI. Bars represent 25 μm. Data represent mean ± SEM. $^{*}p<0.05$ compared to saline; $^{\#}p<0.05$ compared to free IRIN; $^{\&}p<0.05$ compared to Onivyde® (1-way ANOVA followed by a Tukey's test).

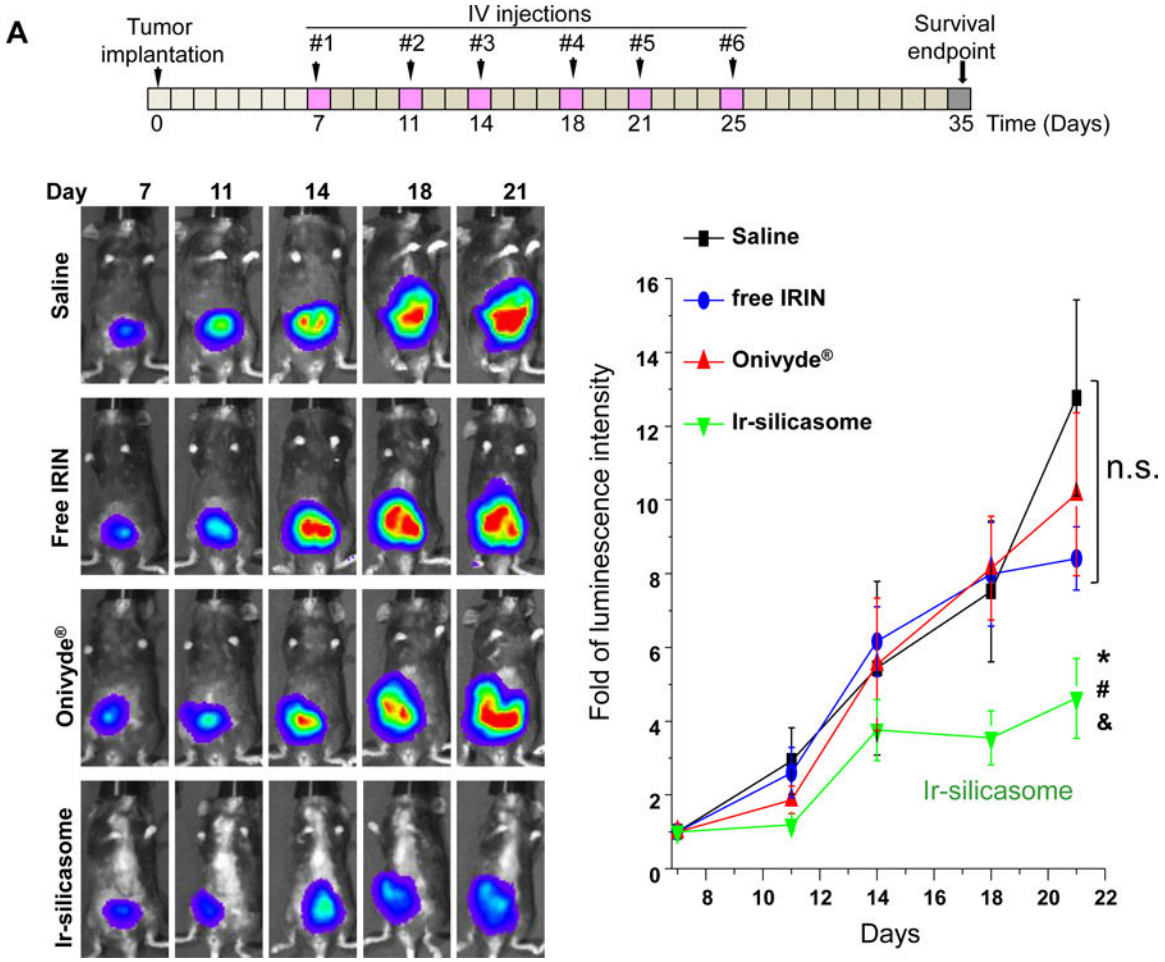

B

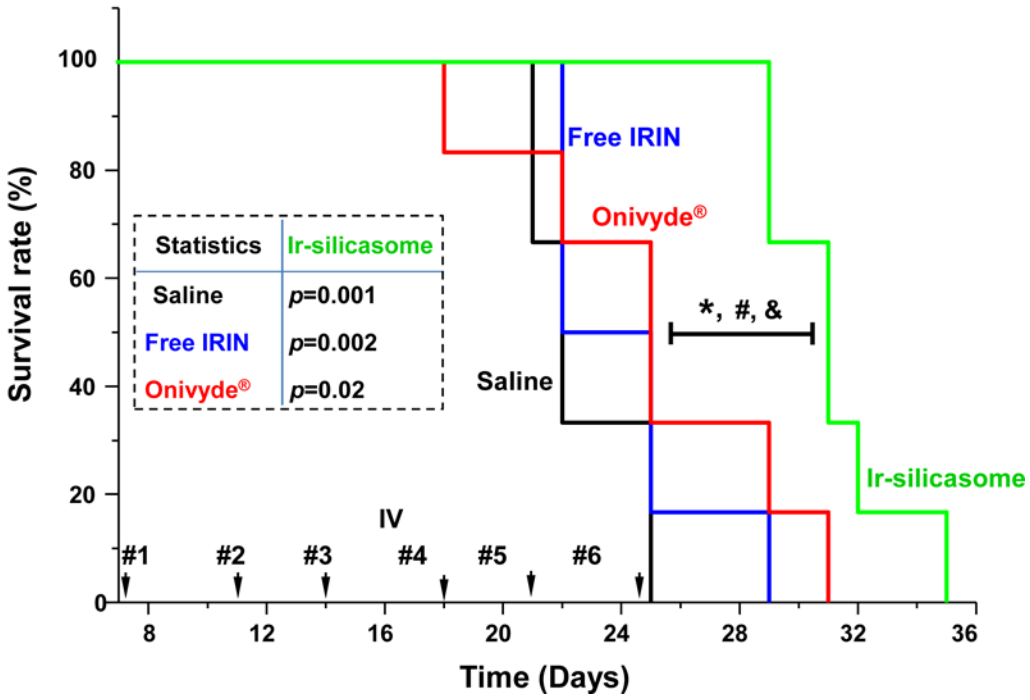

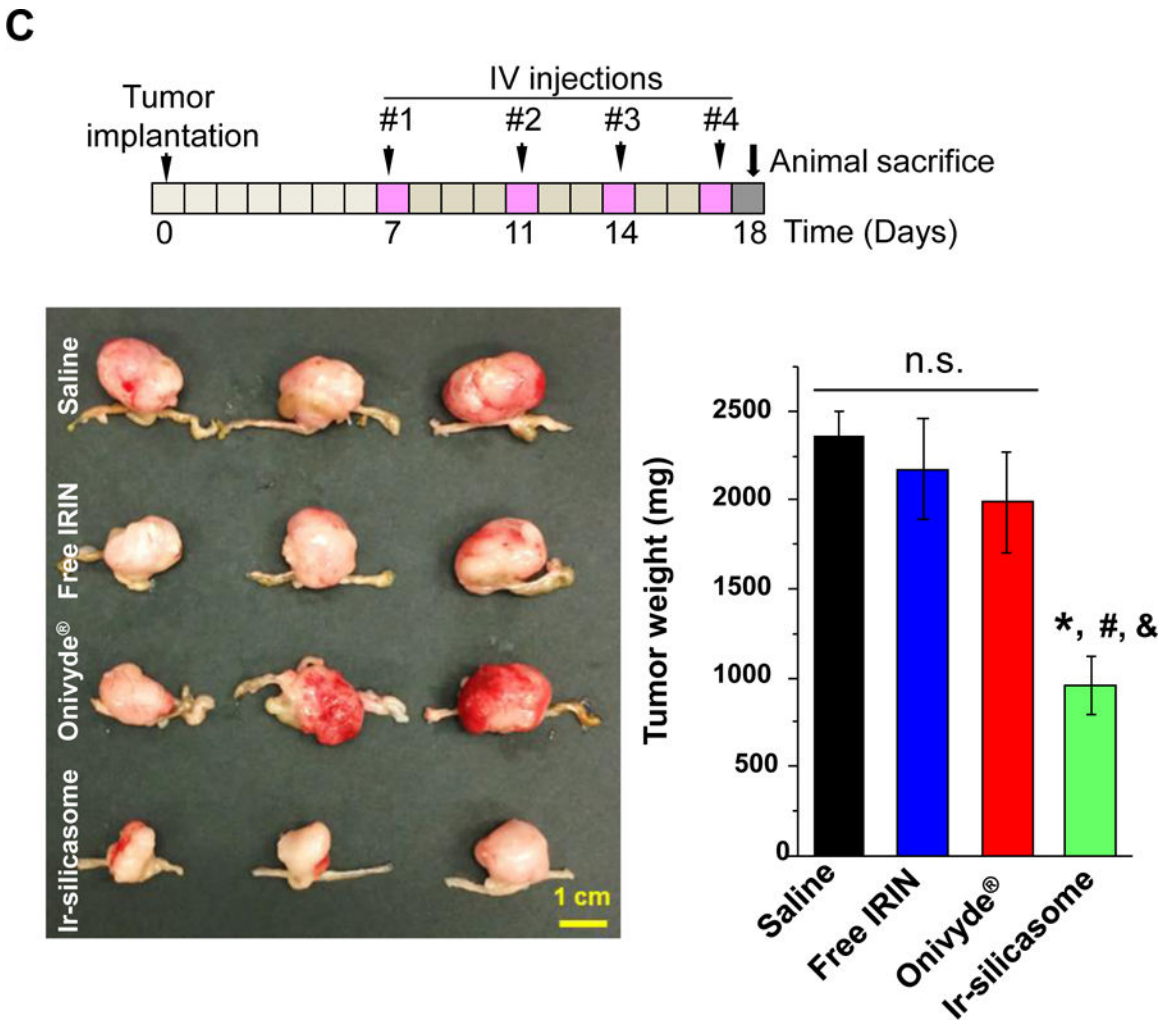

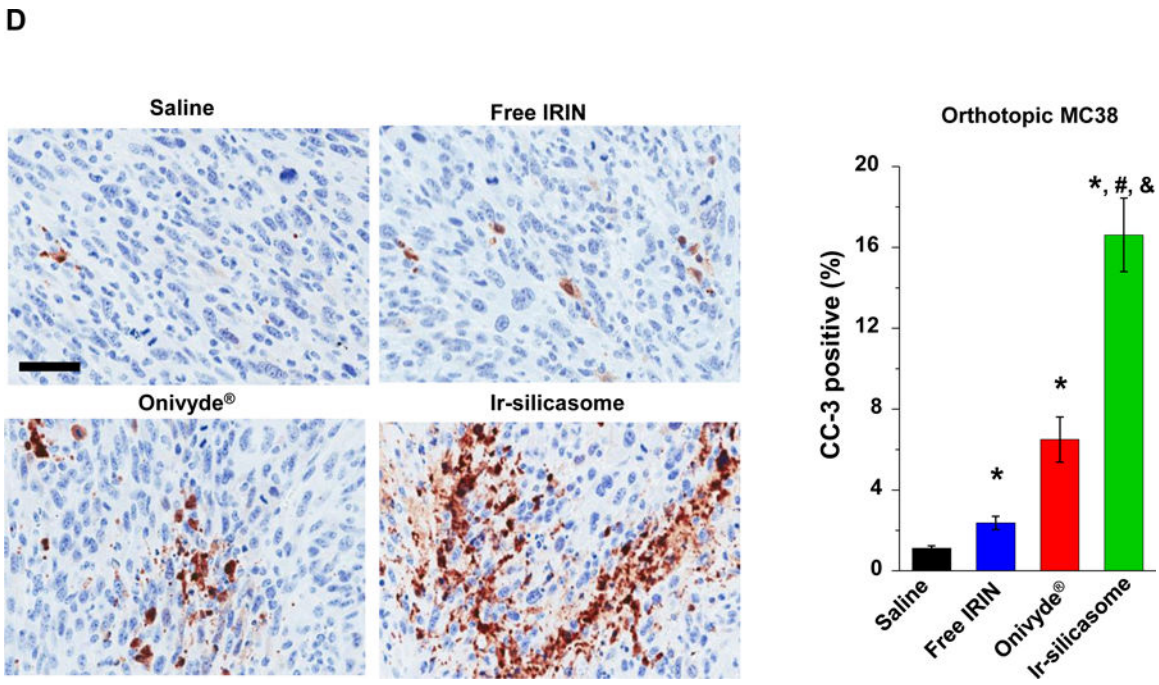

Figure 4. Comparative efficacy testing of the Ir-silicasome in the orthotopic MC38 model.

(A) A survival experiment was performed, in the course of which IVIS imaging was used to compare tumor growth up to day 21, beyond which metastatic peritoneal spread interfered in image detection. MC38 tumor-bearing mice (n = 6) received free irinotecan, Onivyde® or Ir-silicasome at an irinotecan dose equivalent of 40 mg/kg twice per week for up to six IV administrations. Saline was used as the negative control. Representative images are shown in the left panel, with quantitative data display of bioluminescence intensity at the ROI, using IVIS software. (B) Kaplan-Meier plots to display the survival rate of the different animal groups in the same experiment (*p<0.05, Log Rank test). (C) In a separate experiment, the tumor-bearing mice received similar doses as in (A) twice a week for a total of four administrations (n = 3). Animals were sacrificed at 24 hr after the last treatment (day 18). Orthotopic tumors were collected and weighed. (D) IHC analysis of cleaved caspase-3 (CC-3) expression in the orthotopic tumors harvested in (C). Quantification of the number of CC-3$^+$ cells, using ImageScope software (right panel). Bar = 100 μm. Data represent mean ± SEM; *p<0.05 compared to saline; $^{\#}p$<0.05 compared to free IRIN; $^{\&}p$<0.05 compared to Onivyde®. “n.s.” indicates p>0.05.

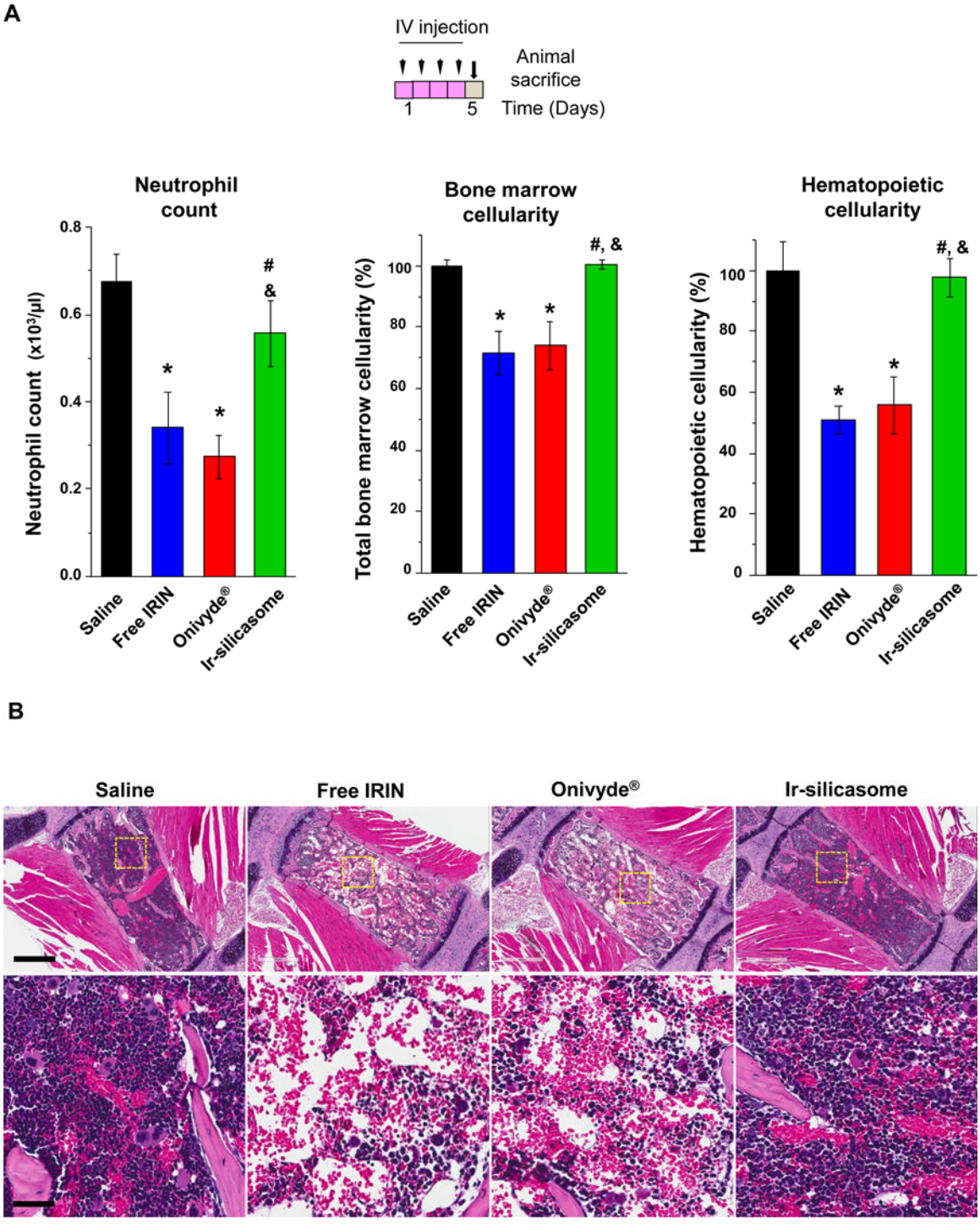

C

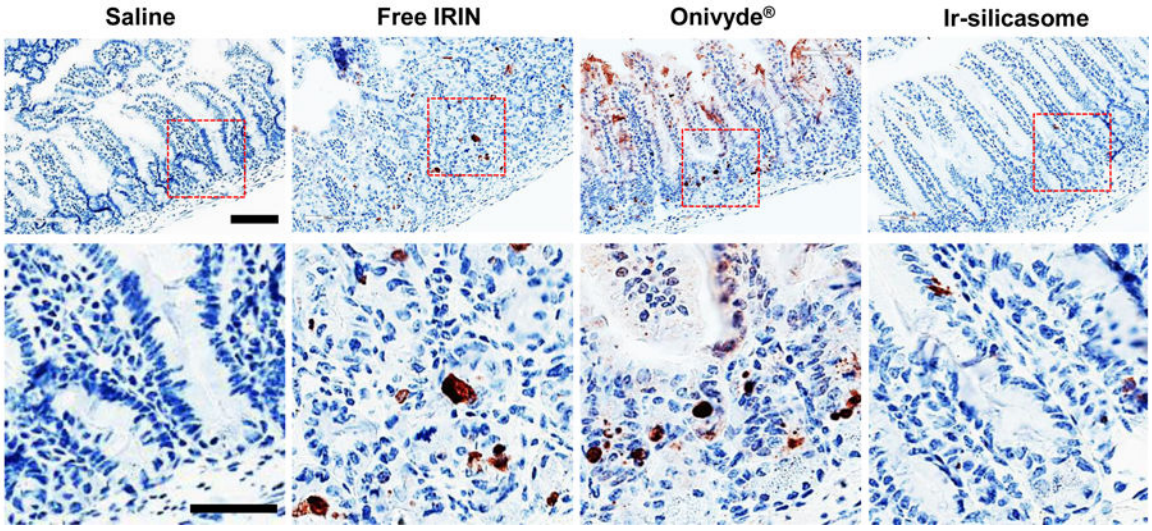

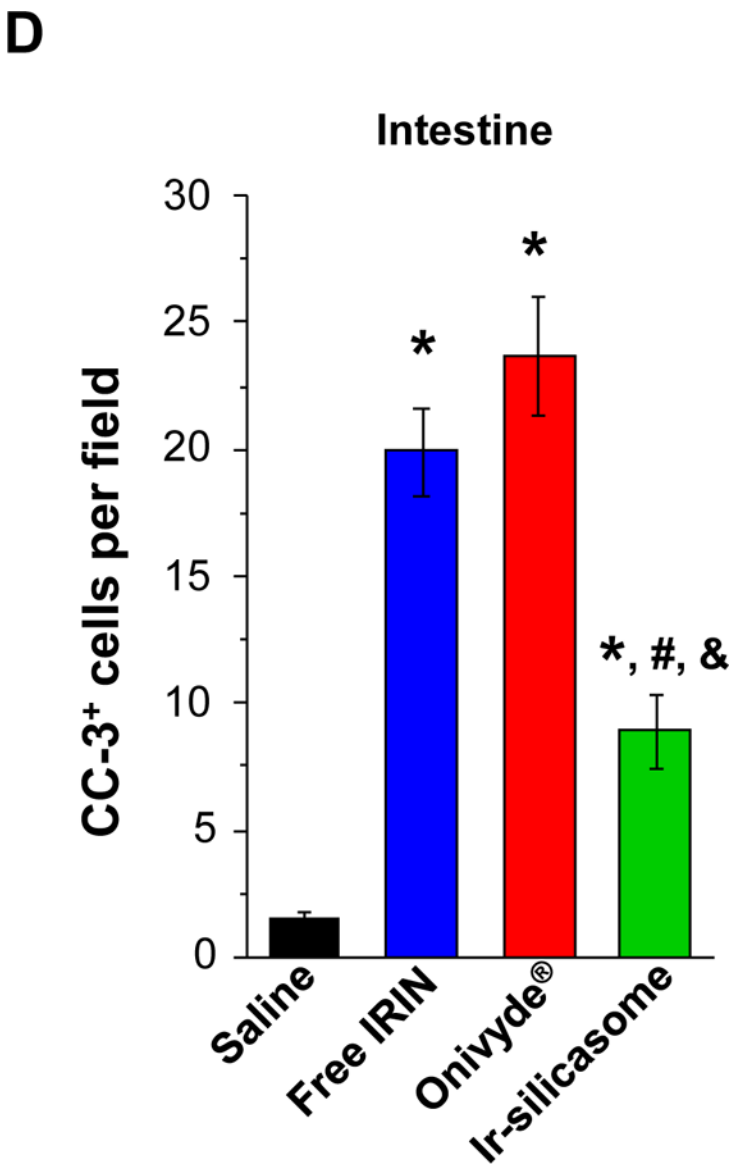

Figure 5. Reduction of bone marrow and GI tract toxicity by encapsulated irinotecan delivery by the silicasome.

(**A**) Peripheral blood was collected to obtain differential WBC and neutrophil counts in non-tumor-bearing animals 24 hr after receiving 4 IV injections of the various irinotecan formulations at 40 mg/kg. Bone marrow toxicity was evaluated by H&E staining of sternal tissue. Normalized total bone marrow cellularity was determined by using Aperio ImageScope software to calculate the surface area occupied by all cell types (middle panel), as well as the surface area occupied by nucleated hematopoietic cells (right panel). **(B)** Representative H&E images of the sternums. Both low (bar = 400 μm) and high (bar = 50 μm) magnification pictures are shown. **(C)** GI tract toxicity evaluated by IHC analysis to discern the number of intestinal groups displaying cleaved caspase-3 (CC-3). The intestines were collected from the experiment in (A). Representative CC-3 IHC staining images in low (bar = 100 μm) and high (bar = 50 μm) magnification are shown. (**D**) Quantitative display of

the percentage CC-3^{+} cells. Data represent mean ± SEM. *p<0.05 compared to saline; $^{\#}p$<0.05 compared to free IRIN; $^{\&}p$<0.05 compared to Onivyde®.

A

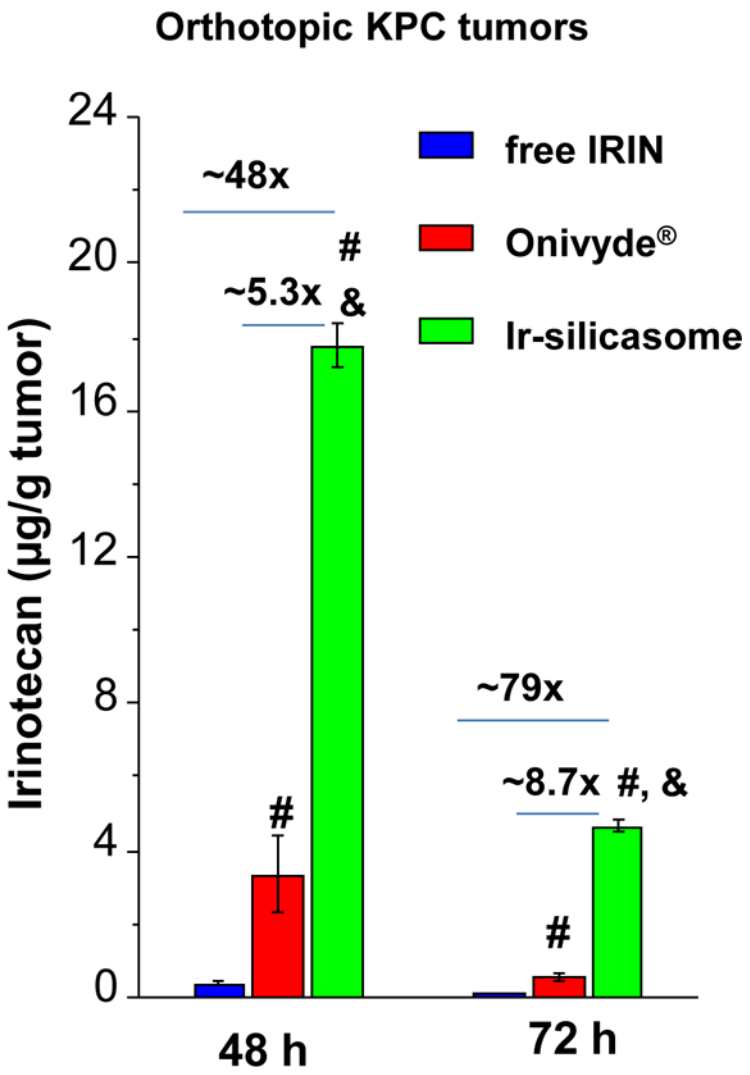

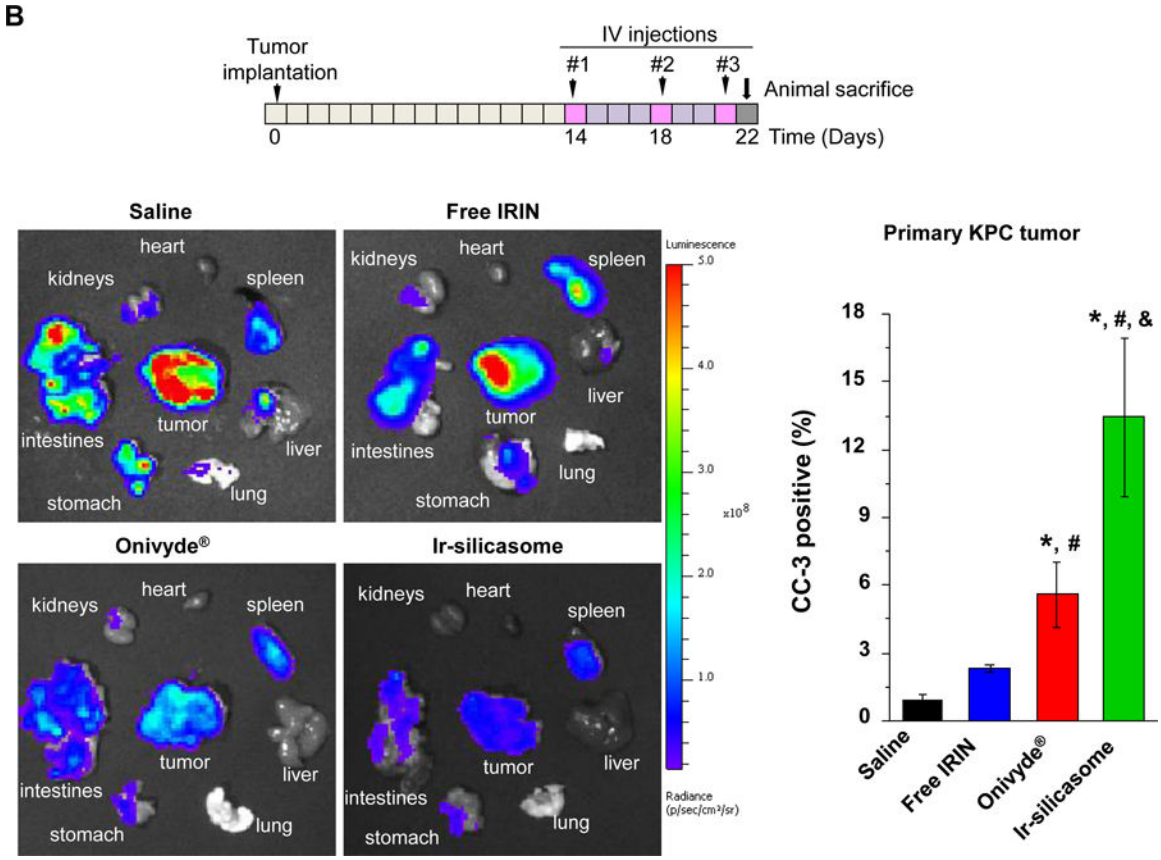

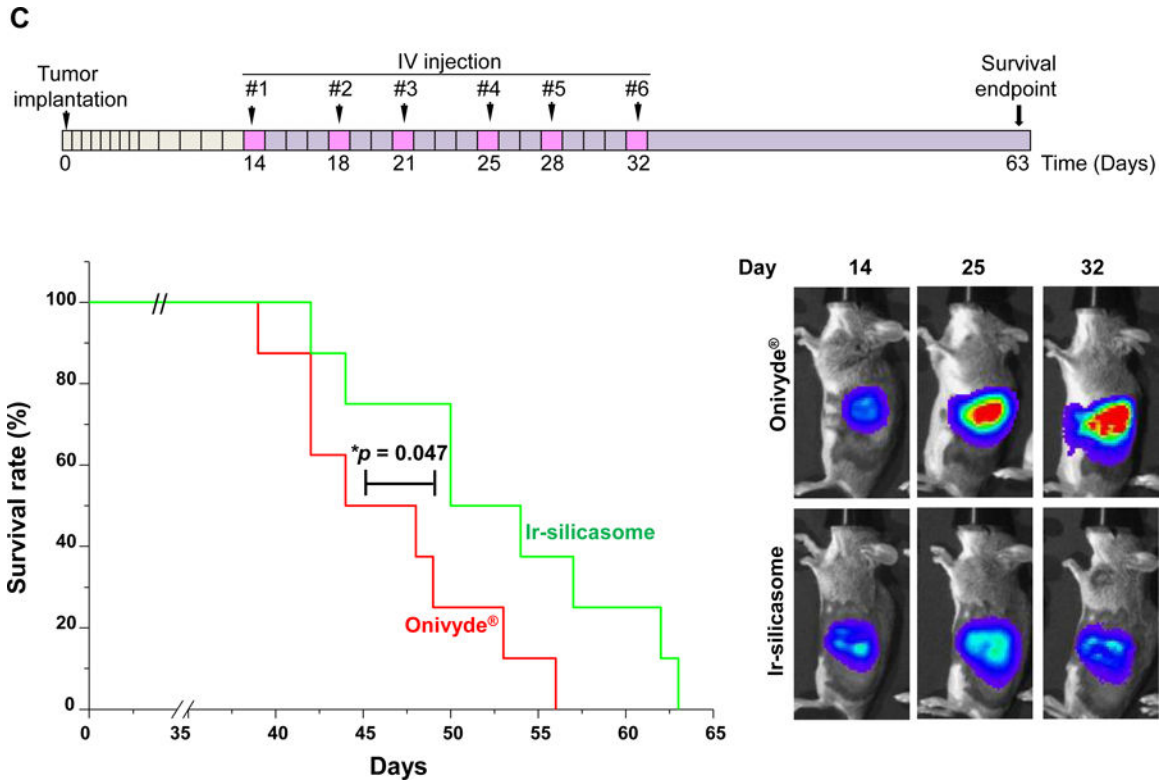

Figure 6. The custom designed Ir-silicasome demonstrate increased efficacy over Onivyde® in an orthotopic PDAC model.

(**A**) Intratumoral irinotecan content in orthotopic KPC tumor bearing mice that received a single IV injection of the Ir-silicasome, Onivyde®, or free drug at an irinotecan dose equivalent of 40 mg/kg. The mice were sacrificed after 48 hr or 72 hr, and irinotecan content at the harvested tumor sites was determined by UPLC-MS as described in Figure 3B. (**B**) Efficacy experiment to compare the effects of various irinotecan formulations on primary tumor growth and metastasis. Orthotopic KPC tumor bearing animals received treatments at an irinotecan dose of 40 mg/kg twice per week or saline, for a total of three IV administrations (n = 3). Animals were sacrificed at 24 h after the last treatment; autopsy and *ex vivo* bioluminescence imaging were performed to evaluate the primary and metastatic tumor burden in each group. IHC analysis of CC-3 was performed on primary tumors. (**C**) An independent experiment was conducted to determine the survival outcome between Ir-silicasome *vs.* Onivyde® (n = 8). Orthotopic KPC-bearing mice received IV injections of an equivalent dose of 40 mg/kg irinotecan twice per week for a total of six administrations. Overall survival rate was determined as described in Figure 4 (left bottom panel, $*p<0.05$, Log Rank test), and orthotopic tumor growth was monitored by live animal tumor bioluminescence imaging (Right bottom panel, Figure S18). Data represent mean ± SEM. $*p<0.05$ compared to saline; $^{\#}p<0.05$ compared to free IRIN; $^{\&}p<0.05$ compared to Onivyde®.